



Conical shell vibration control with distributed piezoelectric sensor and actuator layer



Rasa Jamshidi ^{*}, A.A. Jafari

Mechanical Engineering Department, K.N. Toosi University of Technology, Tehran, Iran

ARTICLE INFO

Keywords:

Conical shell
Piezoelectric layer
Distributed actuator/sensor
Vibration

ABSTRACT

In this study, a simply supported conical shell with distributed piezoelectric sensor and actuator layers is considered and the shell's vibration reduction is investigated. Four kinds of piezoelectric layer distribution which are upper circumferential, middle circumferential, lower circumferential, and longitudinal distribution are considered. The output voltage of each piezoelectric sensor patch which is proportional to the shell deformation is calculated. A PD controller is considered which magnifies sensor output voltage and applies it on the allocated piezoelectric actuator patch. By this method the amplitude of conical shell vibration reduced. The effect of a distributed sensor and actuator on the conical shell vibration is evaluated. Controller type, controller constant, sensor/actuator distributions effectiveness on the free vibration response, the frequency response is evaluated. The results show that derivative controllers can affect more on natural frequencies of conical shells and it can increase the damping of the structure. The circumferential distribution can change natural frequencies easily and it has more effects on the dynamic of the conical shell than longitudinal distribution, especially the lower circumferential distribution. The maximum voltage for the piezoelectric actuator patch is also calculated and better distribution with lower actuator voltage and higher vibration reduction is chosen.

1. Introduction

High amount of undesirable vibrations in structures can easily cause catastrophic failures. Hence, these kinds of noises and vibrations should be avoided as long as it is possible. However, this condition in some structures cannot be avoided and it is inevitable. In this case, the structure should be designed carefully to be more resilient in facing undesirable vibrations. A drawback of this method is the increase in the structure's mass which can be an obstacle in lightweight structures. Another way for avoiding high amount of vibrations, which has become very popular these days, is called smart structures. Smart structures can sense the structure's deformations and produce proportional forces in the opposite direction to compensate unwelcomed vibrations. In these kinds of structures, a distributed sensor can measure structure displacement in any important location with higher accuracy. Additionally, a controller with a variety of controller constants can be used. Similarly, in these structures, a distributed actuator can produce distributed forces which can reduce undesired vibrations smoothly. The need for these structures is increasing especially in the aviation industry where the mass of the structure plays a crucial role in its performance.

Smart structures can be used in many cases and there are many different kinds of smart structures which can avoid a large number of vibrations. However, piezoelectric layers are the most common and useful smart structures which can be used as a sensor, actuator and even energy harvester. In this study piezoelectric layers are used to measure vibrations and compensate them in conical shells. The sensor piezoelectric layer measures the structure deformation and it feedbacks it to the controller as a voltage signal. After magnifying the voltage signal by the controller, it is applied to the actuator piezoelectric layer to compensate the undesired vibrations.

There are many pieces of research about structures with piezoelectric layers e.g. a beam with a piezoelectric layer, a plate with piezoelectric patches and similarly a cylindrical shell with piezoelectric layers. However, studies about conical shells with piezoelectric layers or patches are very rare and this field has not been studied thoroughly. The reason for this is the complexity of the conical shell structures which makes it demanding to analyze. Adding a piezoelectric layer to the conical shell increases the structural complexity which makes it implausible to analyze. Therefore, a few numbers of studies about conical shells with the piezoelectric layer are done until now and they are summarized here.

* Corresponding author.

E-mail address: rs.jamshidi@mail.kntu.ac.ir (R. Jamshidi).

Optimal vibration control of conical shells with collocated helical sensor/actuator pairs was studied by Li et al [1]. The piezoelectric sensor/actuator layer was distributed helically and the conical shell boundary condition was clamped free. The analysis was carried on the modal space and the proposed system was investigated in each mode, separately. The dynamics of a conical shell with a piezoelectric layer were not shown, explicitly. The results could only show piezoelectric layer effects on each mode response separately. Thereby, it couldn't demonstrate the total dynamic response of the shell, vividly. Li et al [2] studied active vibration control of conical shells using ceramic piezoelectric materials. Only an actuator piezoelectric patch with a derivative controller was considered and conical shell undesired vibrations were decreased. The effect of piezoelectric layer distribution was not discussed.

There are some studies concerning conical shells with a piezoelectric sensor layer or actuator layer. These studies are not related to this research directly, but they are worth mentioning and some of them are discussed here.

Tzou et al [3] evaluated distributed actuation characteristics of conical shells with full and diagonal actuators. They used the finite element method and forces distributed actuators on the conical shell surface were evaluated. Spatial microscopic actuations of shallow conical shell sections with free-free boundary conditions were investigated by Chai et al [4]. The entire shell surface was covered with the piezoelectric layer and segmented into patches and forces of each patch were computed. Micro-actuation characteristics of rocket conical shell sections with free-free boundary conditions were studied by Chai et al [5]. Li et al [6] evaluated distributed actuation characteristics of clamped-free conical shells using diagonal piezoelectric actuators. Jamshidi and Jafari [7] studied actuator piezoelectric layer distribution on conical shell surface and actuator forces in each mode of vibration were calculated. Three kinds of distributions which were circumferential, longitudinal and diagonal were considered and the effect of piezoelectric layer distribution on actuator forces was evaluated. Effect of conic angle, piezoelectric layer thickness and its segmentations on actuator forces were also discussed.

Li et al [8] derived modal signals of torsion and transverse sensing of clamped-free conical shells. The conical shell distributed sensing characteristics were evaluated by Tzou et al [3]. They separated the sensing signals of each mode into four components, related to the four-strain items, i.e., the longitudinal membrane strain, the circumferential membrane strain, the longitudinal bending strain, and the circumferential bending strain. Chai et al [9] studied neural potentials and micro-signals of non-linear deep and shallow conical shells with free-free boundary conditions. The dominating signal component among the four contributing micro-signal components was the circumferential membrane component. Jamshidi and Jafari [10] evaluated piezoelectric sensor distribution on conical shells with simply supported boundary conditions. Three kinds of piezoelectric layer distribution were considered and the effect of it on sensor output signal was evaluated. Also, the effect of cone angle, piezoelectric layer thickness, cone length and piezoelectric layer segmentation on sensor output signals were evaluated. In another study, Jamshidi, and Jafari [11] studied transverse sensing of the conical shell with a full surface covered piezoelectric layer. All of the conical shell surfaces were covered with a sensor piezoelectric layer and it was segmented into patches. The output sensor voltage of each patch was calculated in each mode shape. The dominant sensor voltage component was identified in simply supported Boundary conditions.

In this inquiry, conical shell vibration mitigation with a sensor and actuator piezoelectric layer which are connected by a proportional derivative controller is investigated. Four kinds of piezoelectric layer distributions (lower circumferential, middle circumferential, upper circumferential and longitudinal distribution) with a PD controller is considered and evaluated. Electromechanical equations of motion conical shells with sensor piezoelectric layer and actuator piezoelectric layer

are extracted for the first time and the producer is described in detail. The sensor patch output signal is extracted from these equations and actuator forces are calculated for any distributions. The Galerkin method is used to solve the complex derived electromechanical equations. Two conical shell model is considered as a case study and the effect of piezoelectric layer distribution and controller constants on the free vibration response, frequency response of conical shells are discussed thoroughly. Additionally, the piezoelectric actuator voltage is calculated in each condition, the better distributions with lower needed actuator voltage and a higher amount of vibration mitigation are chosen.

2. Strain displacement relations

In this section, conical shell strain displacement relations and mechanical membrane and bending forces are described. A typical conical shell with corresponding curvilinear coordinates is considered and presented in Fig. 1. The conical shell is assumed to be thin. At first, it is assumed that the structure has a piezoelectric sensor patch attached to the top of the conical shell and a piezoelectric actuator patch attached to the under of conical shell. The geometry of the actuator patch and its location is presumed to be the same as the sensor patch.

Considering Kirchhoff-Love assumption, in-plane displacements and linear vibrations, strain displacement relations for the conical shells are obtained.

$$\varepsilon_{xx} = \varepsilon_{xx}^0 + zk_{xx} \quad (1.a)$$

$$\varepsilon_{\theta\theta} = \varepsilon_{\theta\theta}^0 + zk_{\theta\theta} \quad (1.b)$$

$$\varepsilon_{x\theta} = \varepsilon_{x\theta}^0 + zk_{x\theta} \quad (1.c)$$

where membrane strains in the conical shells are defined as [7]:

$$\varepsilon_{xx} = \frac{\partial u}{\partial x} \quad (2.a)$$

$$\varepsilon_{\theta\theta}^0 = \frac{u}{x} + \frac{1}{x \sin(\psi)} \frac{\partial v}{\partial \theta} + \frac{w}{x \tan(\psi)} \quad (2.b)$$

$$\varepsilon_{x\theta}^0 = \frac{1}{x \sin(\psi)} \frac{\partial u}{\partial \theta} - \frac{v}{x} + \frac{\partial v}{\partial x} \quad (2.c)$$

where u , v and w are displacements in the x , θ and z directions, respectively (Fig. 1) and ψ is the cone angle. Similarly bending strains relations in thin conical shells are presumed as [7]:

$$k_{xx} = -\frac{\partial^2 w}{\partial x^2} \quad (3.a)$$

$$k_{\theta\theta} = \frac{\cos(\psi)}{(x \sin(\psi))^2} \frac{\partial v}{\partial \theta} - \frac{1}{(x \sin(\psi))^2} \frac{\partial^2 w}{\partial \theta^2} - \frac{1}{x} \frac{\partial w}{\partial x} \quad (3.b)$$

$$k_{x\theta} = \frac{1}{x \tan(\psi)} \frac{\partial v}{\partial x} - \frac{2v}{x^2 \tan(\psi)} - \frac{2}{x \sin(\psi)} \frac{\partial^2 w}{\partial x \partial \theta} + \frac{2}{x^2 \sin(\psi)} \frac{\partial w}{\partial \theta} \quad (3.c)$$

Mechanical membrane/bending forces for conical shells can be derived from mechanical stresses which in turn have relations with the structure strains.

$$N_{xx}^m = \int_0^h \sigma_{xx}^m dz = K(\varepsilon_{xx}^0 + \nu \varepsilon_{\theta\theta}^0) \quad (4.a)$$

$$N_{\theta\theta}^m = \int_0^h \sigma_{\theta\theta}^m dz = K(\varepsilon_{\theta\theta}^0 + \nu \varepsilon_{xx}^0) \quad (4.b)$$

$$N_{x\theta}^m = \int_0^h \sigma_{x\theta}^m dz = \frac{K(1-\nu)}{2} \varepsilon_{x\theta}^0 \quad (4.c)$$

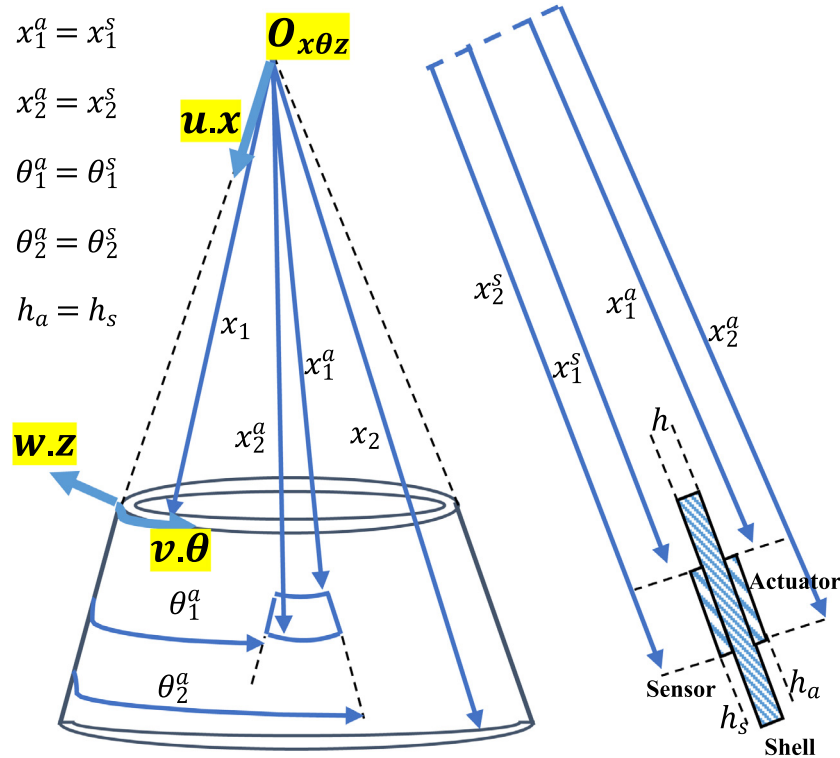


Fig. 1. Thin conical shell with a piezoelectric sensor patch and a piezoelectric actuator patch.

$$M_{xx}^m = \int_0^h \sigma_{xx}^m z dz = D(k_{xx} + \nu k_{\theta\theta}) \quad (4.d)$$

$$M_{\theta\theta}^m = \int_0^h \sigma_{\theta\theta}^m z dz = D(k_{\theta\theta} + \nu k_{xx}) \quad (4.e)$$

$$M_{x\theta}^m = \int_0^h \sigma_{x\theta}^m z dz = \frac{D(1-\nu)}{2} k_{x\theta} \quad (4.f)$$

where $K = \frac{Eh}{1-\nu^2}$ and $D = \frac{Eh^3}{12(1-\nu^2)}$ are shell membrane and bending stiffness, respectively and h is the shell thickness. Considering these strains and membrane/bending forces, conical shell with piezoelectric layer electromechanical equations of motions are extracted.

3. Conical shell electro-mechanical equations of motion

In this section a conical shell with an actuator piezoelectric layer and a sensor piezoelectric layer is considered and electromechanical equations of motion of this system are extracted. The polarization direction is considered to be along Z-axis (Fig. 2).

The in-plane electric fields E_x and E_θ are neglected and only transverse electric field E_z is considered.

$$E_x = E_\theta = 0, E_z = -\frac{\partial \phi}{\partial z} \quad (5)$$

Based on the proposed assumptions, the conical shell electromechanical motion equations in three directions with sensor equations are extracted. The procedure is too long and it is described separately in appendix A in detail. The piezoelectric layer thickness is considered to be neglectable in comparison with conical shell thickness. Therefore, the inertial terms and mechanical stiffness terms related to piezoelectric layers are neglected for simplicity of analysis. The electromechanical equations of motion of conical shells with two piezoelectric layers are extracted and presented in Eq. (6).

$$\frac{\partial N_{xx}^m}{\partial x} + \frac{N_{xx}^m - N_{\theta\theta}^m}{x} + \frac{1}{x \sin(\psi)} \frac{\partial N_{x\theta}^m}{\partial \theta} + q_x = I_o \ddot{u} + \frac{\partial N_{xx}^e}{\partial x} + \frac{N_{xx}^e - N_{\theta\theta}^e}{x} \quad (6.a)$$

$$\begin{aligned} & \frac{\partial N_{x\theta}^m}{\partial x} + \frac{2}{x} N_{x\theta}^m + \frac{1}{x \sin(\psi)} \frac{\partial N_{\theta\theta}^m}{\partial \theta} + \frac{1}{x \tan(\psi)} \frac{\partial M_{x\theta}^m}{\partial x} + \frac{2}{x^2 \tan(\psi)} M_{x\theta}^m \\ & + \frac{\cos(\psi)}{(x \sin(\psi))^2} \frac{\partial M_{\theta\theta}^m}{\partial \theta} + q_\theta \\ & = I_o \ddot{v} + \frac{1}{x \sin(\psi)} \frac{\partial M_{\theta\theta}^e}{\partial \theta} + \frac{\cos(\psi)}{(x \sin(\psi))^2} \frac{\partial M_{\theta\theta}^e}{\partial \theta} \end{aligned} \quad (6.b)$$

$$\begin{aligned} & \frac{\partial^2 M_{xx}^m}{\partial x^2} + \frac{2}{x} \frac{\partial M_{xx}^m}{\partial x} - \frac{N_{\theta\theta}^m}{x \tan(\psi)} + \frac{1}{(x \sin(\psi))^2} \frac{\partial^2 M_{\theta\theta}^m}{\partial \theta^2} - \frac{1}{x} \frac{\partial M_{\theta\theta}^m}{\partial x} \\ & + \frac{2}{x \sin(\psi)} \frac{\partial^2 M_{x\theta}^m}{\partial x \partial \theta} + \frac{2}{x^2 \sin(\psi)} \frac{\partial M_{x\theta}^m}{\partial \theta} + q_z \\ & = I_o \ddot{w} + \frac{\partial^2 M_{xx}^e}{\partial x^2} + \frac{2}{x} \frac{\partial M_{xx}^e}{\partial x} - \frac{N_{\theta\theta}^e}{x \tan(\psi)} + \frac{1}{(x \sin(\psi))^2} \frac{\partial^2 M_{\theta\theta}^e}{\partial \theta^2} - \frac{1}{x} \\ & \times \frac{\partial M_{\theta\theta}^e}{\partial x} \end{aligned} \quad (6.c)$$

$$\frac{\partial}{\partial z} (e_{31} \epsilon_{xx} + e_{32} \epsilon_{\theta\theta} + e_{33} E_z) = 0 \quad (6.d)$$

where q_x , q_θ and q_z are external mechanical forces applied to the conical shell in longitudinal, circumferential and transverse directions, respectively. Also I_o is the inertial term of conical shell which is presented in Appendix A. Furthermore, N_{xx}^e and $N_{\theta\theta}^e$ are electrical membrane forces and similarly M_{xx}^e and $M_{\theta\theta}^e$ are electrical bending forces which are defined as:

$$N_{xx}^e = d_{31} E_p \phi^a(t) [u(x - x_1^a) - u(x - x_2^a)] [u(\theta - \theta_1^a) - u(\theta - \theta_2^a)] \quad (7.a)$$

$$N_{\theta\theta}^e = d_{32} E_p \phi^a(t) [u(x - x_1^a) - u(x - x_2^a)] [u(\theta - \theta_1^a) - u(\theta - \theta_2^a)] \quad (7.b)$$

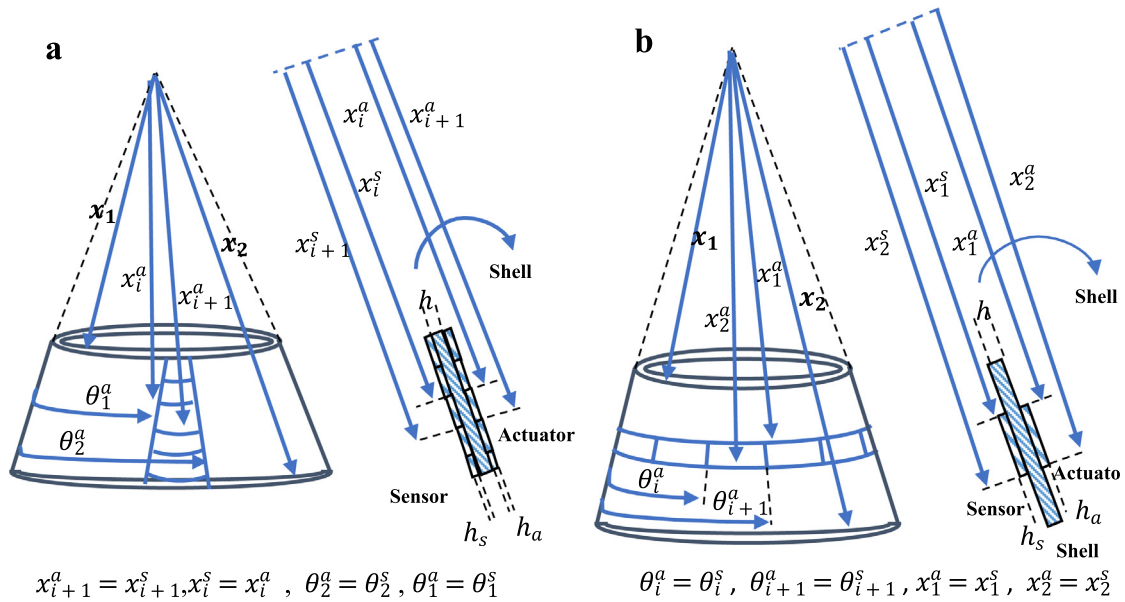


Fig. 2. Thin conical shell with a sensor and an actuator layer a) Longitudinal distribution b) Circumferential distribution.

$$M_{xx}^e = r_x^a d_{31} E_p \phi^a(t) [u(x - x_1^a) - u(x - x_2^a)] [u(\theta - \theta_1^a) - u(\theta - \theta_2^a)] \quad (7.c)$$

$$M_{\theta\theta}^e = r_\theta^a d_{32} E_p \phi^a(t) [u(x - x_1^a) - u(x - x_2^a)] [u(\theta - \theta_1^a) - u(\theta - \theta_2^a)] \quad (7.d)$$

where d_{31} and d_{32} are piezoelectric constants, r_x^a and r_θ^a are the distance between actuator electric neutral layer and conical shell neutral layer. E_p is actuator elastic module and $\phi^a(t)$ is applied actuator voltage. The piezoelectric actuator patch is distributed in the longitudinal direction from x_1^a to x_2^a and in the circumferential direction from θ_1^a to θ_2^a .

The first three equations in Eq. (6) are electromechanical equations of motion in three directions. The left part of these equations is related to the structural stiffness and external mechanical forces on the structure and the right parts of these equations are related to inertial terms of conical shell and electrical actuator forces. The fourth equation in Eq. (6) represents the sensor equation and from that, the sensor output signal can be calculated. This signal is feedbacked to a controller where an amplifier magnifies it. Then, the magnified signal is imported to the collocated actuator patch which can apply forces to the shell for compensating undesired vibrations.

4. Sensor output signal

In this section, the sensor output signal is calculated from Eq. (6.d). From this equation, it can be concluded that:

$$\phi^s = \frac{h_s}{S_e} \int_{x_1^s}^{x_2^s} \int_{\theta_1^s}^{\theta_2^s} \left[h_{31} \left(\frac{\partial u}{\partial x} - z \frac{\partial^2 w}{\partial x^2} \right) + h_{32} \left(\frac{u}{x} + \frac{1}{x \sin(\psi)} \frac{\partial v}{\partial \theta} + \frac{w}{x \tan(\psi)} + z \left(\frac{\cos(\psi)}{(x \sin(\psi))^2} \frac{\partial v}{\partial \theta} - \frac{1}{x \sin(\psi)} \frac{\partial^2 w}{\partial \theta^2} - \frac{1}{x} \frac{\partial w}{\partial x} \right) \right) \right] x \sin(\psi) d\theta dx \quad (8)$$

$$e_{31}\varepsilon_{xx} + e_{32}\varepsilon_{\theta\theta} + e_{33}E_z = 0 \quad (8)$$

Considering Eq. (5), the Eq. (8) can be written as:

$$\frac{\partial \phi}{\partial z} = \frac{e_{31}}{e_{33}} \varepsilon_{xx} + \frac{e_{32}}{e_{33}} \varepsilon_{\theta\theta} \quad (9)$$

Integrating this equation's both sides leads to:

$$\phi = \int_0^{h_s} \left(\frac{e_{31}}{e_{33}} \varepsilon_{xx} + \frac{e_{32}}{e_{33}} \varepsilon_{\theta\theta} \right) dz = h_s \left(\frac{e_{31}}{e_{33}} \varepsilon_{xx} + \frac{e_{32}}{e_{33}} \varepsilon_{\theta\theta} \right) \quad (10)$$

where h_s is piezoelectric sensor layer thickness. Acknowledging the fact that, the sensor layer is distributed on the shell surface, for calculating the output voltage of a sensor patch, which is distributed in the longitudinal direction from x_1^s to x_2^s and in the circumferential direction from θ_1^s to θ_2^s , an averaging method in the patch surface should be done. To simplify this equation, it is considered that $\frac{e_{31}}{e_{33}} = h_{31}$ and $\frac{e_{32}}{e_{33}} = h_{32}$. Therefore, the output voltage of a distributed sensor patch can be calculated by:

$$\phi^s = \frac{h_s}{S_e} \int_{x_1^s}^{x_2^s} \int_{\theta_1^s}^{\theta_2^s} (h_{31} \varepsilon_{xx} + h_{32} \varepsilon_{\theta\theta}) dS_e$$

where S_e is the sensor patch surface area and it is calculated by:

$$S_e = \int_{x_1^s}^{x_2^s} \int_{\theta_1^s}^{\theta_2^s} x \sin(\psi) d\theta dx = \frac{1}{2} (x_2^s)^2 - (x_1^s)^2 (\theta_2^s - \theta_1^s) \sin(\psi) \quad (12)$$

Considering Eqs. (1) and (11), the sensor output signal equation can be developed as:

$$\phi^s = \frac{h_s}{S_e} \int_{x_1^s}^{x_2^s} \int_{\theta_1^s}^{\theta_2^s} (h_{31} (\varepsilon_{xx}^0 + zk_{xx}) + h_{32} (\varepsilon_{\theta\theta}^0 + zk_{\theta\theta})) x \sin(\psi) d\theta dx \quad (13)$$

In the above equation, strain terms can be written by displacement terms (Eqs. (2) and (3)). Then, the sensor output signal equation can be developed as:

$$\phi^s = \frac{h_s}{S_e} \int_{x_1^s}^{x_2^s} \int_{\theta_1^s}^{\theta_2^s} \left(h_{31} \left(\varepsilon_{xx}^0 + z \frac{\partial u}{\partial x} \right) + h_{32} \left(\varepsilon_{\theta\theta}^0 + z \frac{\partial v}{\partial \theta} \right) \right) x \sin(\psi) d\theta dx \quad (14)$$

Conical shell boundary condition is considered to be simply supported at both ends. The mode shape functions of the conical shell with simply supported boundary conditions are considered as:

$$U(x, \theta, t) = \sum_{m=1}^{\infty} \sum_{n=1}^{\infty} \cos\left(\frac{m\pi(x - x_1)}{x_2 - x_1}\right) \cos(n\theta) \eta_{xmn}(t) \quad (15a)$$

$$V(x, \theta, t) = \sum_{m=1}^{\infty} \sum_{n=1}^{\infty} \sin\left(\frac{m\pi(x - x_1)}{x_2 - x_1}\right) \sin(n\theta) \eta_{\theta mn}(t) \quad (15b)$$

$$W(x, \theta, t) = \sum_{m=1}^{\infty} \sum_{n=1}^{\infty} \sin\left(\frac{m\pi(x - x_1)}{x_2 - x_1}\right) \cos(n\theta) \eta_{zmn}(t) \quad (15c)$$

where x_1 and x_2 are the upper and lower dimensions of the truncated conical shell (Fig. 1). Due to the complexity of the sensor output voltage equation, it is separated into four parts which are: the longitudinal membrane strain voltage ($\phi_{exx_i}^s$), the circumferential membrane strain voltage ($\phi_{e\theta\theta_i}^s$), the longitudinal bending strain voltage ($\phi_{kx_i}^s$) and the circumferential bending strain voltage ($\phi_{k\theta_i}^s$). Considering the proposed mode shape functions, each sensor patch output voltage regarding separated parts are presented here:

$$\phi_i^s = \phi_{exx_i}^s + \phi_{kx_i}^s + \phi_{e\theta\theta_i}^s + \phi_{k\theta_i}^s \quad (16a)$$

$$\phi_{exx_i}^s = -\frac{h_s h_{31}}{S_{ei}} \sin(\psi) \left[\sum_{m=1}^{\infty} \sum_{n=1}^{\infty} \eta_{xmn}(t) \left(\frac{m\pi}{x_2 - x_1} \right) \int_{x_i}^{x_{i+1}} \int_{\theta_i}^{\theta_{i+1}} x \sin\left(\frac{m\pi(x - x_1)}{x_2 - x_1}\right) \cos(n\theta) d\theta dx \right] \quad (16b)$$

$$\phi_{kx_i}^s = \frac{r_s^2 h_s h_{31}}{S_{ei}} \sin(\psi) \left[\sum_{m=1}^{\infty} \sum_{n=1}^{\infty} \eta_{zmn}(t) \left(\frac{m\pi}{x_2 - x_1} \right)^2 \int_{x_i}^{x_{i+1}} \int_{\theta_i}^{\theta_{i+1}} x \sin\left(\frac{m\pi(x - x_1)}{x_2 - x_1}\right) \cos(n\theta) d\theta dx \right] \quad (16c)$$

$$\phi_{e\theta\theta_i}^s = \frac{h_s h_{32}}{S_{ei}} \left[\sum_{m=1}^{\infty} \sum_{n=1}^{\infty} \eta_{\theta mn}(t) \int_{x_i}^{x_{i+1}} \int_{\theta_i}^{\theta_{i+1}} \cos\left(\frac{m\pi(x - x_1)}{x_2 - x_1}\right) \cos(n\theta) \sin(\psi) d\theta dx + (\eta_{\theta mn}(t) + \cos(\psi) \eta_{zmn}(t)) \int_{x_i}^{x_{i+1}} \int_{\theta_i}^{\theta_{i+1}} \frac{1}{x} \sin\left(\frac{m\pi(x - x_1)}{x_2 - x_1}\right) \cos(n\theta) d\theta dx - \eta_{zmn}(t) \sin(\psi) \left(\frac{m\pi}{x_2 - x_1} \right) \int_{x_i}^{x_{i+1}} \int_{\theta_i}^{\theta_{i+1}} \cos\left(\frac{m\pi(x - x_1)}{x_2 - x_1}\right) \cos(n\theta) d\theta dx \right] \quad (16d)$$

(16e) where ϕ_i^s is the i th patch output sensor signal. Using Eq. (16), the sensor output voltage of all patches in any kind of distribution can be calculated. This voltage has a relation with conical shell deformation and thereby it can represent the amount of conical shell deformation.

5. Controller design

In this section, a controller is considered for determining the relationship between the sensor output voltage and applied actuator voltage. Due to the complexity of motion equations, a classic and simple controller is considered which decreases the complexity and makes it possible to solve. A proportional derivative controller is considered by which for each patch, an independent controller constant is determined. This controller defines each actuator patch applied signal, which is related to the collocated sensor output voltage.

$$\phi_i^a(t) = -\left(K_{p_i} \phi_i^s(t) + K_{d_i} \frac{d\phi_i^s(t)}{dt}\right) \quad (17)$$

So, each actuator applied signal is defined and by that actuator forces will be determined.

6. Actuator forces

In the next step, distributed piezoelectric actuator forces with defined applied voltage are extracted. The actuator membrane forces and bending moments described in Eq. (7) are for a single actuator patch. If there are n_p numbers of actuator patches on the distributed piezoelectric layer, the actuator forces and bending moments will be considered as the summation of all the patches forces and bending moments which is determined by:

$$N_{xx}^e = -d_{31} E_p \times \sum_{i=1}^{n_p} \phi_i^a [u(x - x_i^a) - u(x - x_{i+1}^a)] [u(\theta - \theta_i^a) - u(\theta - \theta_{i+1}^a)] \quad (18a)$$

$$N_{\theta\theta}^e = -d_{32} E_p \times \sum_{i=1}^{n_p} \phi_i^a [u(x - x_i^a) - u(x - x_{i+1}^a)] [u(\theta - \theta_i^a) - u(\theta - \theta_{i+1}^a)] \quad (18b)$$

$$M_{xx}^e = -r_x^a d_{31} E_p \times \sum_{i=1}^{n_p} \phi_i^a [u(x - x_i^a) - u(x - x_{i+1}^a)] [u(\theta - \theta_i^a) - u(\theta - \theta_{i+1}^a)] \quad (18c)$$

$$M_{\theta\theta}^e = -r_\theta^a d_{32} E_p \times \sum_{i=1}^{n_p} \phi_i^a [u(x - x_i^a) - u(x - x_{i+1}^a)] [u(\theta - \theta_i^a) - u(\theta - \theta_{i+1}^a)] \quad (18d)$$

As it is shown in the controller equation (Eq. (17)), the applied actuator signal is related to the collocated sensor output signal. Therefore, considering Eqs. (17) and (18), actuator forces can be extracted based on the sensor output signal.

$$N_{xx}^e = -d_{31} E_p \times \sum_{i=1}^{n_p} \left(K_{p_i} \phi_i^s(t) + K_{d_i} \frac{d\phi_i^s(t)}{dt} \right) [u(x - x_i^a) - u(x - x_{i+1}^a)] [u(\theta - \theta_i^a) - u(\theta - \theta_{i+1}^a)] \quad (19a)$$

$$N_{\theta\theta}^e = -d_{32} E_p \times \sum_{i=1}^{n_p} \left(K_{p_i} \phi_i^s(t) + K_{d_i} \frac{d\phi_i^s(t)}{dt} \right) [u(x - x_i^a) - u(x - x_{i+1}^a)] [u(\theta - \theta_i^a) - u(\theta - \theta_{i+1}^a)] \quad (19b)$$

$$M_{xx}^e = -r_x^a d_{31} E_p \times \sum_{i=1}^{n_p} \left(K_{p_i} \phi_i^s(t) + K_{d_i} \frac{d\phi_i^s(t)}{dt} \right) [u(x - x_i^a) - u(x - x_{i+1}^a)] [u(\theta - \theta_i^a) - u(\theta - \theta_{i+1}^a)] \quad (19c)$$

$$M_{\theta\theta}^e = -r_\theta^a d_{32} E_p \times \sum_{i=1}^{n_p} \left(K_{p_i} \phi_i^s(t) + K_{d_i} \frac{d\phi_i^s(t)}{dt} \right) [u(x - x_i^a) - u(x - x_{i+1}^a)] [u(\theta - \theta_i^a) - u(\theta - \theta_{i+1}^a)] \quad (19d)$$

So, the electrical membrane forces and bending moments are calculated by Eq. (19). In electromechanical equations of motion, derivations of these terms exist. These derivatives are extracted and given in Eq. (20).

$$\frac{\partial N_{xx}^e}{\partial x} = -d_{31} E_p \times \sum_{i=1}^{n_p} \left(K_{p_i} \phi_i^s(t) + K_{d_i} \frac{d\phi_i^s(t)}{dt} \right) [\delta(x - x_i^a) - \delta(x - x_{i+1}^a)] [u(\theta - \theta_i^a) - u(\theta - \theta_{i+1}^a)] \quad (20a)$$

$$\frac{\partial N_{\theta\theta}^e}{\partial \theta} = -d_{32} E_p \times \sum_{i=1}^{n_p} \left(K_{p_i} \phi_i^s(t) + K_{d_i} \frac{d\phi_i^s(t)}{dt} \right) [u(x - x_i^a) - u(x - x_{i+1}^a)] [\delta(\theta - \theta_i^a) - \delta(\theta - \theta_{i+1}^a)] \quad (20b)$$

$$\frac{\partial M_{xx}^e}{\partial x} = -r_x^a d_{31} E_p \times \sum_{i=1}^{n_p} \left(K_{pi} \phi_i^s(t) + K_{di} \frac{d\phi_i^s(t)}{dt} \right) [\delta(x - x_i^a) - \delta(x - x_{i+1}^a)] [u(\theta - \theta_i^a) - u(\theta - \theta_{i+1}^a)] \quad (20c)$$

$$\frac{\partial M_{\theta\theta}^e}{\partial \theta} = -r_\theta^a d_{32} E_p \times \sum_{i=1}^{n_p} \left(K_{pi} \phi_i^s(t) + K_{di} \frac{d\phi_i^s(t)}{dt} \right) [u(x - x_i^a) - u(x - x_{i+1}^a)] [\delta(\theta - \theta_i^a) - \delta(\theta - \theta_{i+1}^a)] \quad (20d)$$

$$\frac{\partial^2 M_{xx}^e}{\partial x^2} = -r_x^a d_{31} E_p \times \sum_{i=1}^{n_p} \left(K_{pi} \phi_i^s(t) + K_{di} \frac{d\phi_i^s(t)}{dt} \right) \frac{\partial}{\partial x} [\delta(x - x_i^a) - \delta(x - x_{i+1}^a)] [u(\theta - \theta_i^a) - u(\theta - \theta_{i+1}^a)] \quad (20e)$$

$$\frac{\partial^2 M_{\theta\theta}^e}{\partial \theta^2} = -r_\theta^a d_{32} E_p \times \sum_{i=1}^{n_p} \left(K_{pi} \phi_i^s(t) + K_{di} \frac{d\phi_i^s(t)}{dt} \right) [u(x - x_i^a) - u(x - x_{i+1}^a)] \frac{\partial}{\partial \theta} [\delta(\theta - \theta_i^a) - \delta(\theta - \theta_{i+1}^a)] \quad (20f)$$

Considering Eqs. (16) and (20), all of the electric terms related to actuator forces and bending moments which have a relation with sensor output signal are extracted. As mentioned before, the sensor output signal is dependent on the conical shell's deformations. Therefore, it can be concluded that by this arrangement, actuator forces, and bending moments will become dependent on the conical shell's surface displacements.

In electromechanical equations of motion, the mechanical terms of the conical shell are dependent on its strains which obviously have relations with conical shell's deformation and as it's mentioned earlier, actuator terms are also dependent on the conical shell's deformation. Therefore, it can be mentioned that all of the terms in the electromechanical equations of motion (Eq. (6.a, b, c)) are dependent on conical shell's deformation, except for external mechanical forces which are applied on the shell. The electromechanical equation of motion is simplified and revised based on the conical shell strains and the sensor output signal and it is presented in Eq. 21.

$$K \left[\frac{\partial \varepsilon_{xx}^0}{\partial x} + \nu \frac{\partial \varepsilon_{\theta\theta}^0}{\partial x} + \frac{1-\nu}{2x \sin(\psi)} \frac{\partial \varepsilon_{x\theta}^0}{\partial \theta} + \frac{1-\nu}{x} (\varepsilon_{xx}^0 - \varepsilon_{\theta\theta}^0) \right] + q_x \\ = \rho h \ddot{u} - E_p \sum_{i=1}^{n_p} \left(K_{pi} \phi_i^s + K_{di} \frac{d\phi_i^s}{dt} \right) \times \left[[d_{31} [\delta(x - x_i^a) - \delta(x - x_{i+1}^a)] + \frac{(d_{31} - d_{32})}{x} [u(x - x_i^a) - u(x - x_{i+1}^a)]] [u(\theta - \theta_i^a) - u(\theta - \theta_{i+1}^a)] \right] \quad (21a)$$

$$K \left[\frac{1-\nu}{2} \frac{\partial \varepsilon_{x\theta}^0}{\partial x} + \frac{1-\nu}{x} \varepsilon_{x\theta}^0 + \frac{\nu}{x \sin(\psi)} \frac{\partial \varepsilon_{xx}^0}{\partial \theta} + \frac{1}{x \sin(\psi)} \frac{\partial \varepsilon_{\theta\theta}^0}{\partial \theta} \right] + D \left[\frac{1-\nu}{2x \tan(\psi)} \frac{\partial k_{x\theta}}{\partial x} + \frac{1-\nu}{x^2 \tan(\psi)} k_{x\theta} + \frac{\cos(\psi)}{(x \sin(\psi))^2} \left[\frac{\partial k_{\theta\theta}}{\partial \theta} + \nu \frac{\partial k_{xx}}{\partial \theta} \right] \right] + q_\theta = \rho h \ddot{v} \\ - \sum_{i=1}^{n_p} \left(K_{pi} \phi_i^s + K_{di} \frac{d\phi_i^s}{dt} \right) \frac{E_p d_{32}}{x \sin(\psi)} [u(x - x_i^a) - u(x - x_{i+1}^a)] [\delta(\theta - \theta_i^a) - \delta(\theta - \theta_{i+1}^a)] \left[1 + \frac{r_\theta^a \cos(\psi)}{x \sin(\psi)} \right] \quad (21b)$$

It is clear, that the obtained equations (Eq. (21)) are very complex, and solving these equations is challenging. To solve these equations, the Galerkin method is used to convert these equations into time-domain equations.

7. The Galerkin method

In this part, the simplified electromechanical equations of motion are solved. For solving such a complicated challenging equations, Galerkin method is utilized. The Galerkin method is applied in three directions of motion equations (Eq. 22).

$$\int_{\theta_1}^{\theta_2} \int_{x_1}^{x_2} e q_1 u dx d\theta = 0 \quad (22.a)$$

$$\int_{\theta_1}^{\theta_2} \int_{x_1}^{x_2} e q_2 v dx d\theta = 0 \quad (22.b)$$

$$\int_{\theta_1}^{\theta_2} \int_{x_1}^{x_2} e q_3 w dx d\theta = 0 \quad (22.c)$$

where eq_1 , eq_2 and eq_3 refers to Eqs. (21.a), (21.b) and (21.c) respectively. After applying the Galerkin method, the electromechanical equations of motion are transformed into time-domain equations and these equations are presented in Eq. 23.

$$[M][X] + [C^e][\dot{X}] + [K][X] + [K^e][X] = [F] \quad (23)$$

where $[X]$ is time-domain deformation vector which is demonstrated in Eq. (24).

$$[X] = \begin{bmatrix} \eta_{x11}(t) \\ \vdots \\ \eta_{xpq}(t) \\ \eta_{\theta11}(t) \\ \vdots \\ \eta_{\thetapq}(t) \\ \eta_{z11}(t) \\ \vdots \\ \eta_{zpq}(t) \end{bmatrix} \quad (24)$$

where p and q are the considered numbers of mode shape terms in Eq. (15) in longitudinal and circumferential directions, respectively. In Eq. (23), the mass matrix is diagonal and symmetric with the size of $3pq \times 3pq$ and the diagonal terms can be calculated by $m_{ii} = \frac{\rho h (x_2 - x_1) \pi}{2}$. Stiffness matrix ($[k]$) is an unsymmetrical matrix that is related to conical shell material and geometrical parameters. $[C_e]$ and $[K_e]$ matrices are dependent on geometrical parameters and actuator/sensor material and controller constants. These matrices are determined by:

$$[C^e] = K_v * K_d * SM \quad (25a)$$

$$[K^e] = K_v * K_p * SM \quad (25b)$$

$$D \left[\frac{\partial^2 k_{xx}}{\partial x^2} + \nu \frac{\partial^2 k_{\theta\theta}}{\partial x^2} + \frac{1}{(x \sin(\psi))^2} \left(\nu \frac{\partial^2 k_{xx}}{\partial \theta^2} + \frac{\partial^2 k_{\theta\theta}}{\partial \theta^2} \right) + \frac{1}{x} \left[(2-\nu) \frac{\partial k_{xx}}{\partial x} + (2\nu-1) \frac{\partial k_{\theta\theta}}{\partial x} \right] \right] + \frac{1-\nu}{x \sin(\psi)} \frac{\partial^2 k_{x\theta}}{\partial x \partial \theta} + \frac{1-\nu}{x^2 \sin(\psi)} \frac{\partial k_{x\theta}}{\partial \theta} - \frac{K}{x \tan(\psi)} \left[\nu \varepsilon_{xx}^0 + \varepsilon_{\theta\theta}^0 \right] + q_z \\ = \rho h \ddot{w} - \sum_{i=1}^{n_p} \left(K_{pi} \phi_i^s + K_{di} \frac{d\phi_i^s}{dt} \right) E_p \left[\left[\frac{2d_{31} r_x^a - d_{32} r_\theta^a}{x} [\delta(x - x_i^a) - \delta(x - x_{i+1}^a)] - \frac{d_{32}}{x \tan(\psi)} [u(x - x_i^a) - u(x - x_{i+1}^a)] \right] [u(\theta - \theta_i^a) - u(\theta - \theta_{i+1}^a)] \right] \\ + r_x^a d_{31} \frac{\partial}{\partial x} [\delta(x - x_i^a) - \delta(x - x_{i+1}^a)] [u(\theta - \theta_i^a) - u(\theta - \theta_{i+1}^a)] + r_\theta^a d_{32} \left[u(x - x_i^a) - u(x - x_{i+1}^a) \right] \frac{\partial}{\partial \theta} [\delta(\theta - \theta_i^a) - \delta(\theta - \theta_{i+1}^a)] \quad (21c)$$

where $([SM])$ is the sensitivity matrix related to sensor patches material properties and geometries with the size of $np \times 3pq$. n_p is the sensor/actuator patches quantity. In fact, by multiplying $([SM])$ matrix into the deformation vector (Eq. (24)) the sensor output signal of each patch can be obtained (Eq. (26.c)). In Eq. (25), K_p matrix is related to distributed actuator material properties and geometries with the size of $3pq \times p$ which is determined by Eq. (20). K_p and K_D are diagonal matrices with the size of $np \times np$ which are related to the proportional and derivative controller, respectively.

$$K_p = \begin{bmatrix} K_{p1} & 0 & \cdots & 0 \\ 0 & K_{p2} & \cdots & \vdots \\ \vdots & \vdots & \ddots & 0 \\ 0 & \cdots & 0 & K_{pn_p} \end{bmatrix} \quad (26.a)$$

$$K_D = \begin{bmatrix} K_{d1} & 0 & \cdots & 0 \\ 0 & K_{d2} & \cdots & \vdots \\ \vdots & \vdots & \ddots & 0 \\ 0 & \cdots & 0 & K_{dn_p} \end{bmatrix} \quad (26.b)$$

$$\begin{bmatrix} \phi^s_1 \\ \phi^s_2 \\ \vdots \\ \phi^s_{n_p} \end{bmatrix} = [SM][X] \quad (26.c)$$

where K_{pn_p} is the proportional controller constant of patch number n_p and K_{dn_p} is derivative controller constant of patch number n_p . Obviously, in Eq. (25) matrix $[C_e]$ is created because of the derivative controller and matrix $[K_e]$ is created because of the proportional controller. By changing K_d , the system damping will change and by changing K_p , the system stiffness will change.

By this method, time equations of the proposed system are determined. For evaluating the effect of the proposed system, free vibration response, and frequency response of conical shells are computed and analyzed.

8. Validation

In this section, the accuracy of the proposed method is evaluated by comparing the results with previous works' results. As mentioned earlier, a well-detailed study concerning conical shell vibration control with the piezoelectric layer has not been investigated, yet. Therefore, for validating the proposed method a paper focused on conical shell vibration response without any piezoelectric layers is chosen. For this aim, natural frequencies of conical shell in simply supported boundary condition are calculated and compared with the results of other researches. For this purpose, three different models of conical shells without any piezoelectric layers which were used in previous studies are considered. The geometrical parameter and material property of these models are presented in Table 1 [12–14].

Table 1
Geometrical and material properties of conical shell models.

	Model No. 1	Model No. 2	Model No. 3
$x_1(m)$	0.6	$\frac{3\sqrt{2}}{10}$	$\frac{3\sqrt{3}}{15}$
$x_2(m)$	0.8	$\frac{4\sqrt{2}}{10}$	$\frac{4\sqrt{3}}{15}$
ψ	$\frac{\pi}{6}$	$\frac{\pi}{4}$	$\frac{\pi}{3}$
$h(mm)$	4	4	4
$E(Gpa)$	70	70	70
$\rho(\frac{kg}{m^3})$	2710	2710	2710

For evaluating the described method, the natural frequency of the conical shell in each model is calculated and afterward the non-dimensional frequency parameter (Eq. (27)) in each mode is computed and compared with other researcher's results.

$$f = \omega_0 x_2 \sin(\psi) \sqrt{\frac{\rho(1 - \nu^2)}{E}} \quad (27)$$

The frequency parameter results of this study and three other researchers are presented in Table 2 for comparing.

Obviously, the result of the present study is very close to the previous researches results. Therefore, the described method accuracy is validated precisely and it can be used for evaluating conical shells with piezoelectric layer dynamic response.

As it is stated earlier, there are some studies concerning conical shells with only distributed piezoelectric sensors or conical shells with only distributed piezoelectric actuators. Using these studies, only the sensor output signal or actuator applied forces can be evaluated and validated. To ensure that the presented research has precise results, these mentioned validations were also has been carried out previously. These validations are presented for further clarification in [7,10]. In the first-mentioned reference [7], the actuator applied force is validated and in the second one [10], the sensor output signal is also justified.

9. Case studies

Considering the proposed system, the system response in different conditions is evaluated in this section. For this purpose, two new conical shell models with a piezoelectric sensor layer and a piezoelectric actuator layer are considered. The geometrical and material properties of determined conical shell models are presented in Table 3. In this study conical shell material is considered to be isotropic. However, particulate composites which have similar characteristics to the isotropic materials can also be used in this study [15]. Therefore, in this study conical shell material can be considered as any isotropic material or particulate composites. The free vibration response and frequency response in controlled and uncontrolled conditions are computed.

The effect of piezoelectric layer distributions and controller constants on the free vibration response and frequency response are evaluated and discussed in detail.

In each considered conical shell model, four kinds of piezoelectric distributions are determined which are named as: 1 – Upper circumferential distribution 2 – Middle circumferential distribution 3 – Lower circumferential distribution 4 – Longitudinal distribution. These distributions are displayed in Fig. 3 for further clarifications.

Clearly, as the piezoelectric layer surface area increases, its ability to absorb harmful vibrations improves. Therefore, for an accurate comparison, in each case of piezoelectric layer distribution, the sensor or actuator layer area is considered to be 10% of the conical shell surface area, in each model. The sensor layer geometry and patch quantities are considered to be the same as the actuator layer geometry and patch quantities, respectively. The sensor output voltage of i th patch is feed-back to the controller and after magnification, the voltage is applied to collocated actuator patch (i th actuator patch number).

In distributed sensors or actuators, symmetricalness causes the sensor observability and actuator controllability to diminish. Therefore, this situation should be avoided to enhance the distributed sensor or actuator performance. For avoiding this condition, the number of each piezoelectric layer patches should be considered as an odd number. For avoiding observability and controllability loss (in circumferential distribution), piezoelectric layer patch quantity is considered to be 11 in each distribution.

Modal displacement function terms in Eq. (15) in each direction are considered to be four ($p = 4$ and $q = 4$). For simplicity in both models, shell material and piezoelectric layer material are considered to be

Table 2

Comparing the frequency parameter between present study and previous researches.

Model No.1				Model No.2				Model No.3				
<i>n</i>	Present Study	[12]	[13]	[14]	Present Study	[12]	[13]	[14]	Present Study	[12]	[13]	[14]
2	0.842052	0.8405	0.8431	0.8420	0.765572	0.7639	0.7642	0.7655	0.634854	0.6342	0.6342	0.6348
3	0.737729	0.7375	0.7416	0.7376	0.721325	0.7204	0.7211	0.7212	0.623871	0.6235	0.6336	0.6238
4	0.636347	0.6368	0.6419	0.6362	0.673994	0.6737	0.6747	0.6739	0.614543	0.6144	0.6146	0.6145
4	0.552931	0.5536	0.5590	0.5528	0.632429	0.6325	0.6336	0.6323	0.611084	0.6111	0.6113	0.6111
5	0.495151	0.4955	0.5008	0.4950	0.603595	0.6037	0.6049	0.6035	0.617066	0.6170	0.6172	0.6171
6	0.466247	0.4661	0.4701	0.4661	0.592080	0.5919	0.5928	0.5921	0.634854	0.6346	0.6347	0.6350
7	0.466092	0.4653	0.4687	0.4660	0.599996	0.5994	0.6005	0.6001	0.665794	0.6651	0.6653	0.6660

Table 3

Geometrical and material parameters of two considered conical shell Models.

	Model No.1	Model No.2
$x_1(\text{m})$	0.6	0.6
$x_2(\text{m})$	0.9	0.9
ψ	$\frac{\pi}{3}$	$\frac{\pi}{4}$
$h(\text{mm})$	4	4
$E(\text{Gpa})$	70	70
$\rho(\frac{\text{Kg}}{\text{m}^3})$	2710	2710
$h_a = h_s(\text{mm})$	0.5	0.5
$d_{31}(\text{v/m})$	2.3×10^{-11}	2.3×10^{-11}
$d_{32}(\text{v/m})$	2.3×10^{-11}	2.3×10^{-11}
$h_{31}(\text{C/N})$	4.32×10^8	4.32×10^8
$h_{32}(\text{C/N})$	4.32×10^8	4.32×10^8

aluminum and PVDF, respectively. However, conical shell material can be considered any isotropic material or any particulate composite material.

The exact longitudinal locations of the piezoelectric layer in the upper circumferential, middle circumferential and lower circumferential distributions are presented in Eqs. (28), (29), and (30), respectively.

$$x_1^a = x_1^a = \frac{3x_1 + x_2}{4} - a \quad (28.a)$$

$$x_2^a = x_2^a = \frac{3x_1 + x_2}{4} + a \quad (28.b)$$

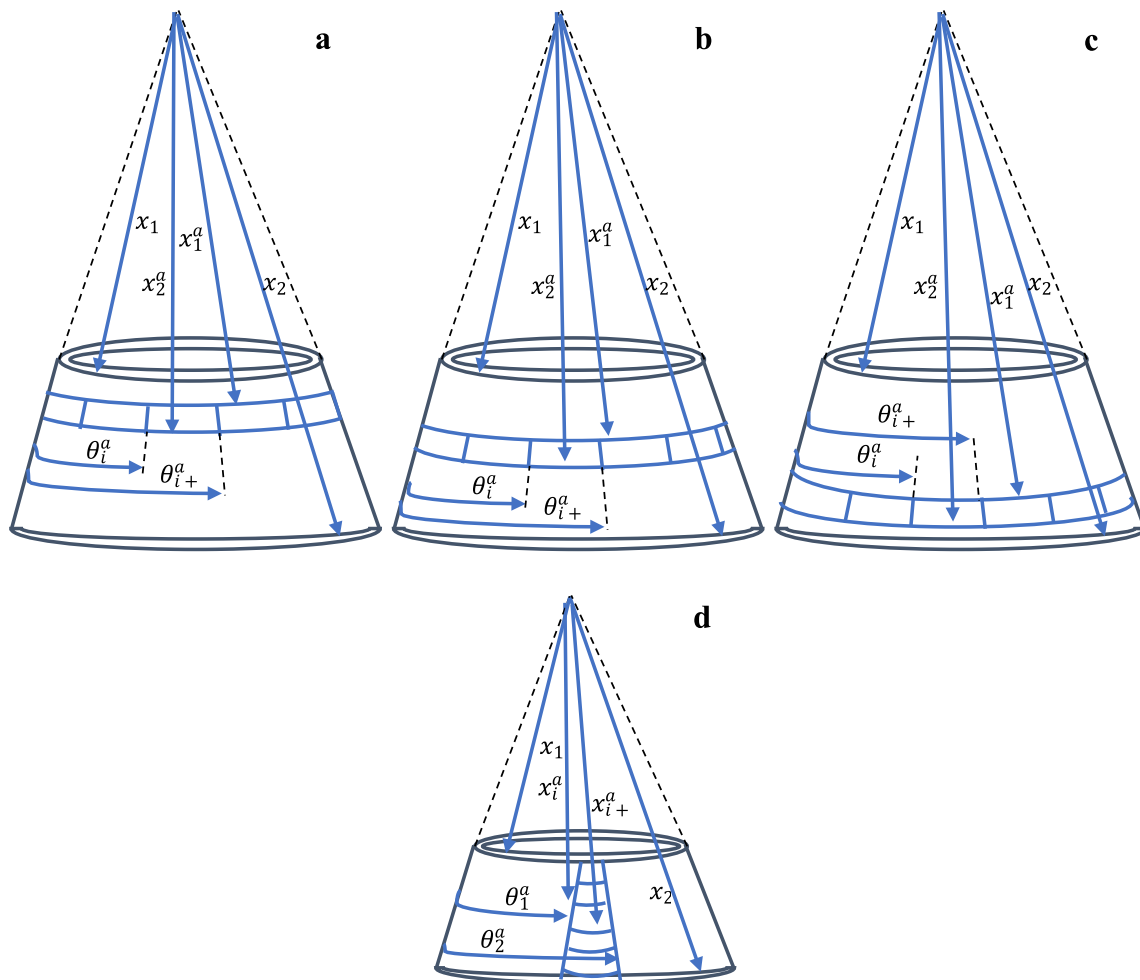


Fig. 3. Thin conical shell with a sensor and an actuator layer with various distributions a) Upper Circumferential distribution b) Middle Circumferential distribution c) Lower Circumferential distribution d) Longitudinal distribution.

$$x_1^s = x_1^a = \frac{x_1 + x_2}{2} - a \quad (29.a)$$

$$x_2^s = x_2^a = \frac{x_1 + x_2}{2} + a \quad (29.b)$$

$$x_1^s = x_1^a = \frac{x_1 + 3x_2}{4} - a \quad (30.a)$$

$$x_2^s = x_2^a = \frac{x_1 + 3x_2}{4} + a \quad (30.b)$$

The a parameter in the above equations are determined in a way that the piezoelectric layer surface area would be the same in each distribution and the magnitude of this parameter is presented in [Table 4](#).

In the longitudinal distribution, the location of piezoelectric layer in circumferential direction is considered as: $\theta_1^s = \theta_1^a = 0$ and $\theta_2^s = \theta_2^a = 0.64$.

The free vibration response and frequency response of considered conical shell models are calculated and presented in the next steps. For determining the effectiveness of the piezoelectric sensor and actuator layer precisely, conical shell response in a controlled condition and uncontrolled condition (without any piezoelectric layer) are calculated and compared with each other in each section. Also, the maximum actuator applied voltage in each response is calculated and presented in each response.

9.1. Free vibration response

In this part, free vibration response of conical shells with distributed piezoelectric sensor and actuator layer for two considered models are computed and evaluated. A small displacement is applied to the conical shell and its response is calculated in both controlled (with piezoelectric layers) and uncontrolled conditions (without any piezoelectric layer) and compared with each other. In each kind of distribution, there are 11 actuator patches and the maximum applied actuator voltage in each case are calculated and presented in each figure separately. In each figure, the transverse displacement is shown with non-dimensional form ($\frac{w}{h}$) in a very short period of time so that the differences between controlled and uncontrolled response can be comparable.

Free vibration response results of conical shell model No.1 with various distributions are presented from [Figs. 4 to 8](#). Similarly, free vibration response results of conical shell model No.2 with various distributions are presented from [Figs. 9 to 13](#).

Obviously, the results indicate that the proposed system has a high capacity in vibration mitigation of conical shells. In all of the presented cases, the response amplitude decreases dramatically by using various piezoelectric layer distribution and controller's constants. Therefore, it can be pointed out that the piezoelectric layer impact on the free vibration mitigation of conical shells is impeccable and it can be used to avoid higher amplitudes.

Piezoelectric layer distribution has an impactful effect on the vibration decline level. Vividly, higher vibration reduction with lower actuator applied voltage is more preferable. By comparing the attained results, the best sensor/actuator distribution can be determined. In the lower circumferential distribution, the vibration reduction is more than other distribution and the applied voltage is less than others. Thereby, this distribution is the best choice in the case of free vibration and simply supported boundary conditions.

Another point which should be mentioned is the effectiveness of controller constants on the vibration level mitigation. Based on the attained results, it can be concluded that the derivative controller has a tremendous effect on reducing the vibration amplitude. On the other hand, the proportional controller doesn't have any significant effect on the vibra-

Table 4
The a Parameter in different circumferential distributions.

	The a parameter (m)
Upper Circumferential	0.0136
Middle Circumferential	0.0150
Lower Circumferential	0.0167

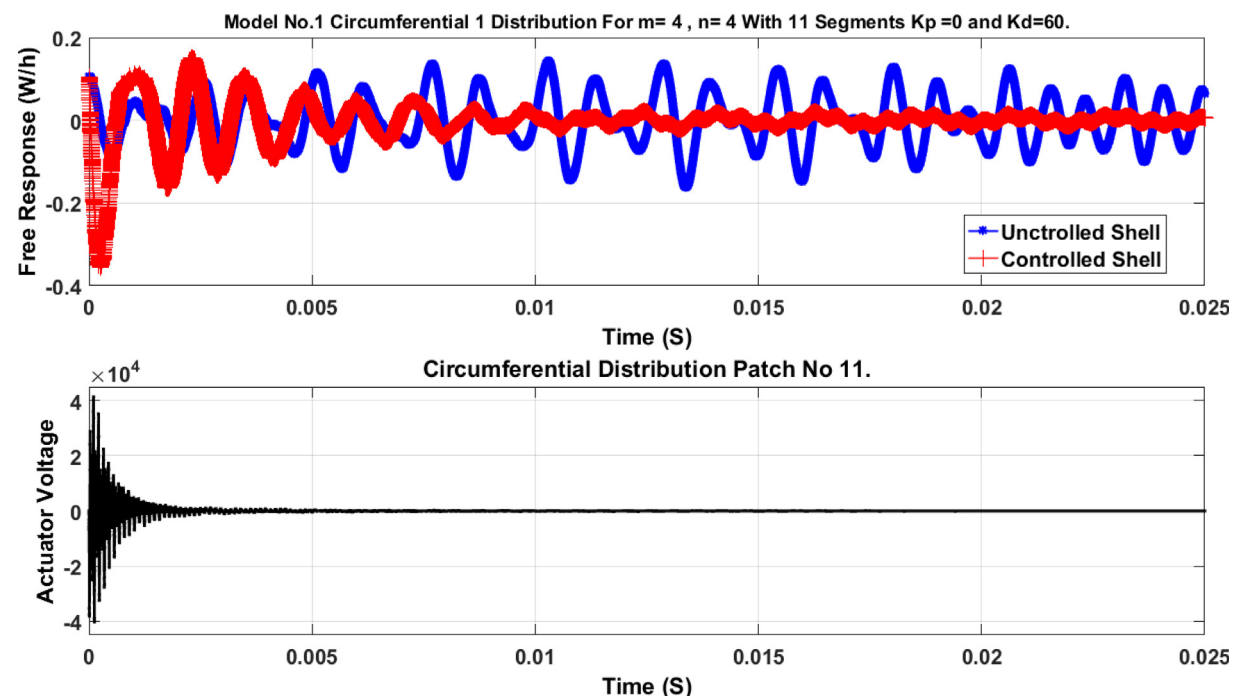


Fig. 4. Free vibration response of model No.1 in upper circumferential distribution with controller constants of $K_p = 0$ and $K_d = 60$. Maximum applied actuator voltage in patch No.11.

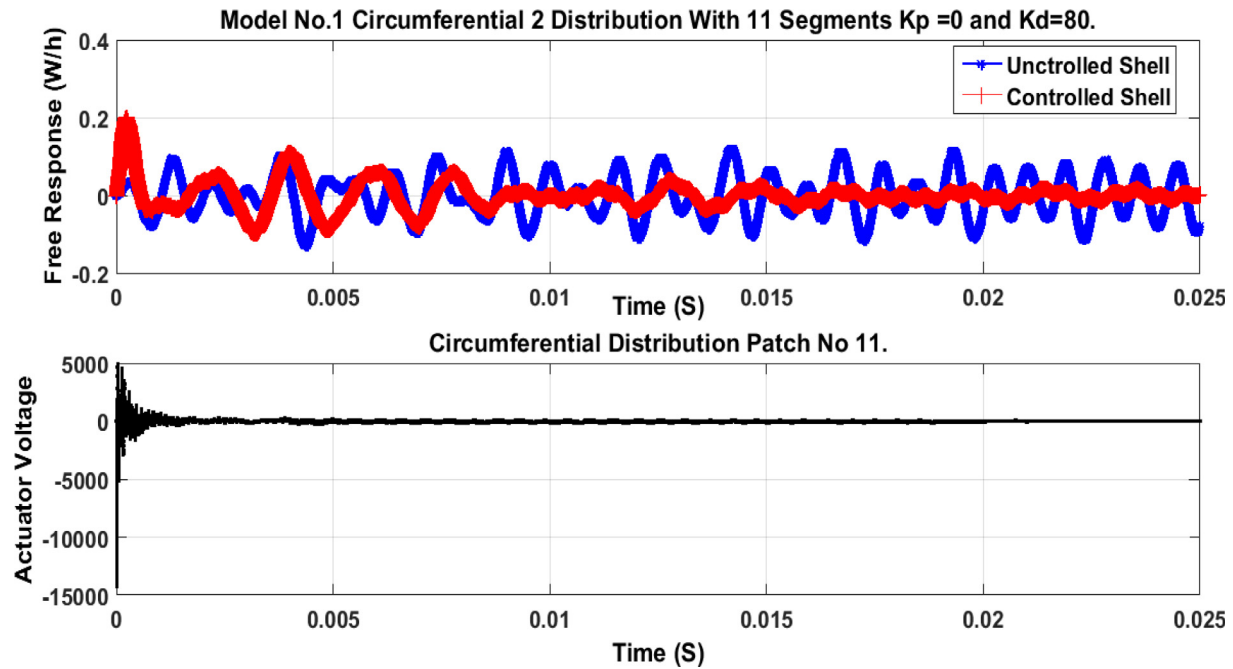


Fig. 5. Free vibration response of model No.1 in middle circumferential distribution with controller constants of $K_p = 0$ and $K_d = 80$. Maximum applied actuator voltage in patch No.11.

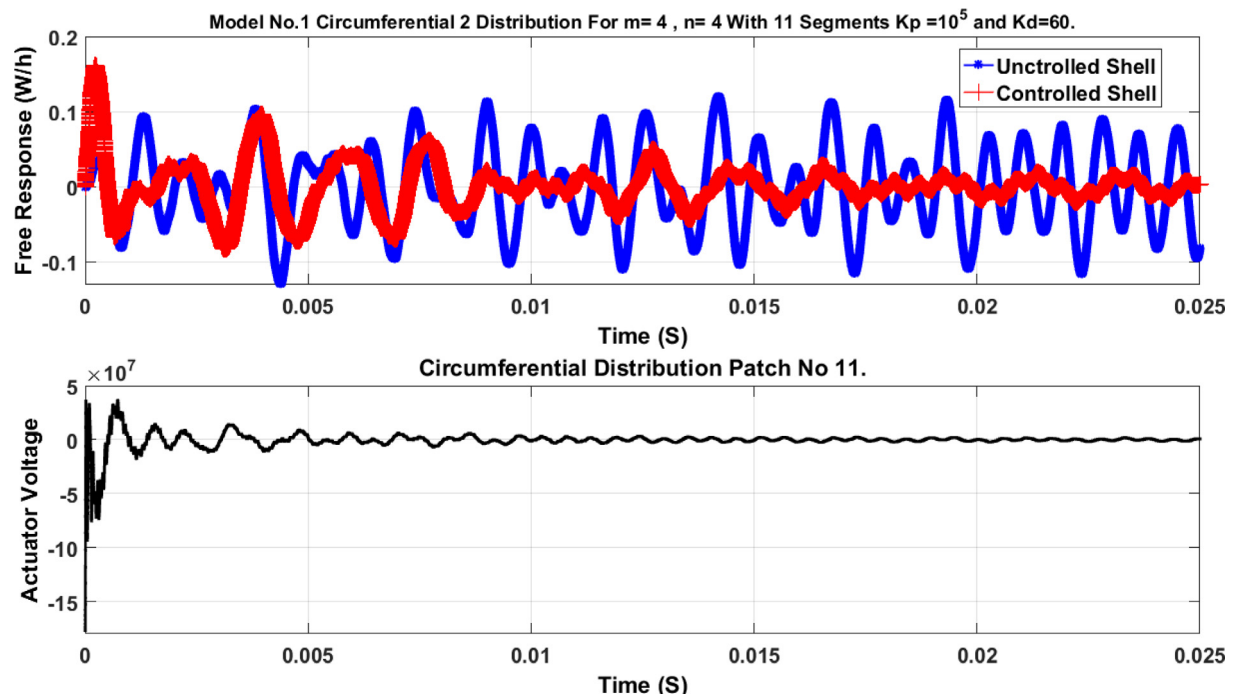


Fig. 6. Free vibration response of model No.1 in middle circumferential distribution with controller constants of $K_p = 10^5$ and $K_d = 60$. Maximum applied actuator voltage in patch No.11.

tion mitigation while it escalates the actuator applied voltage signal. Therefore, for vibration reduction derivative controller is a preferable choice, while the proportional controller is not recommended.

9.2. Frequency response

The frequency response of two considered conical shell models are presented and evaluated in this section. By this method, the effect of

distributed sensor/actuator layer and controller constants on the frequency response can be determined vividly.

For computing the structure frequency response, an external harmonic load in the transverse directions is applied to the conical shell and the amplitude response in the transverse direction is calculated in each excitation frequency step. The excitation frequency range of the externally applied force is considered to be from 0 to 10 kHz and the amplitude of response in each step is computed. By these

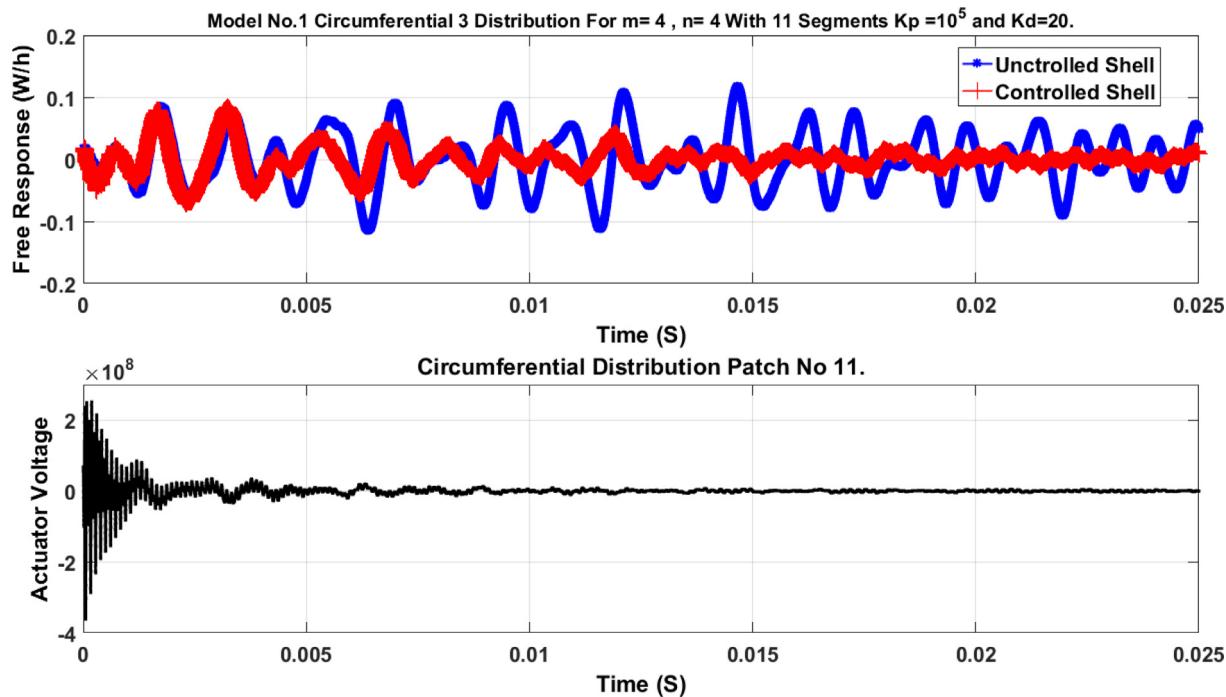


Fig. 7. Free vibration response of model No.1 in lower circumferential distribution with controller constants of $K_p = 10^5$ and $K_d = 20$. Maximum applied actuator voltage in patch No.11.

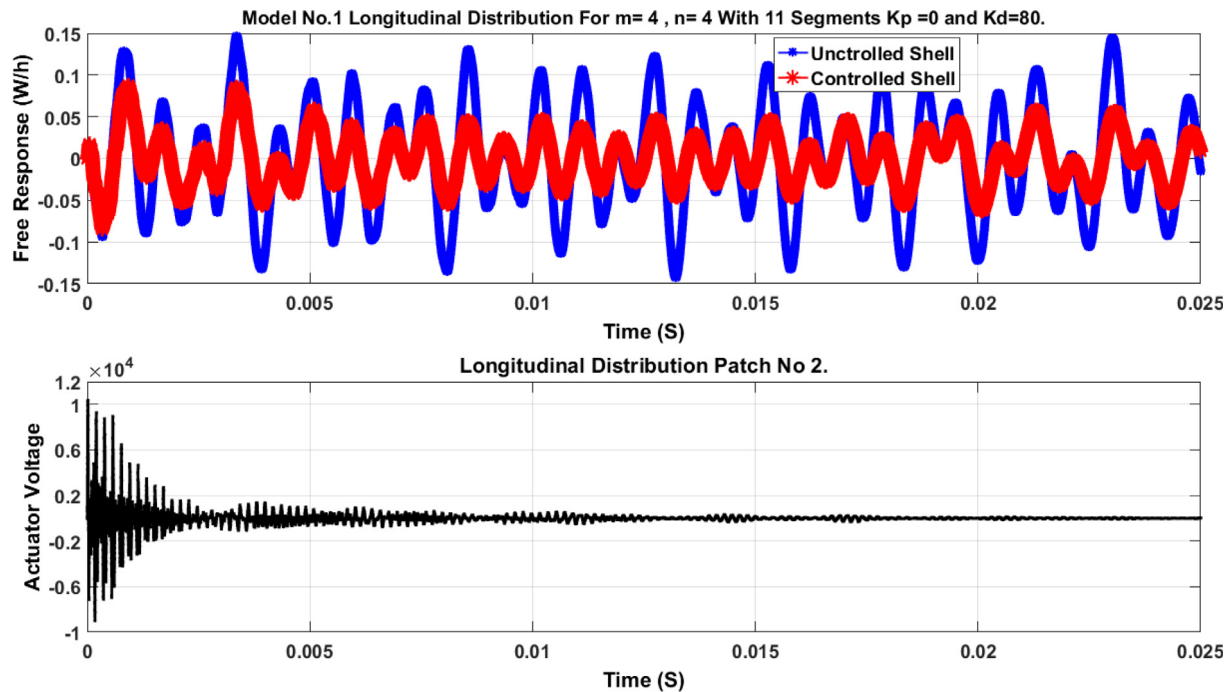


Fig. 8. Free vibration response of model No.1 in longitudinal distribution with controller constants of $K_p = 0$ and $K_d = 80$. Maximum applied actuator voltage in patch No.2.

results, the effect of controller constants and piezoelectric layer distribution on conical shell frequency response can be evaluated, easily.

Frequency response results of conical shell model No.1 with various distributions are presented from Figs. 14 to 18. Similarly, frequency response results of conical shell model No.2 with various distributions are presented from Figs. 19 to 23.

As stated earlier, the proportional controller can increase the structural stiffness and therefore this kind of controller would increase the

natural frequencies of the structure. Likewise, a derivative controller can increase the structural damping and it would decrease the amplitude of the frequency response.

Clearly, the high effect of piezoelectric layers on the frequency response of conical shells are undeniable. The frequency response amplitude of the controlled shell is obviously lower than the frequency response amplitude of the uncontrolled shell. So, by using the proposed system, vibration amplitude of structure can be decreased dra-

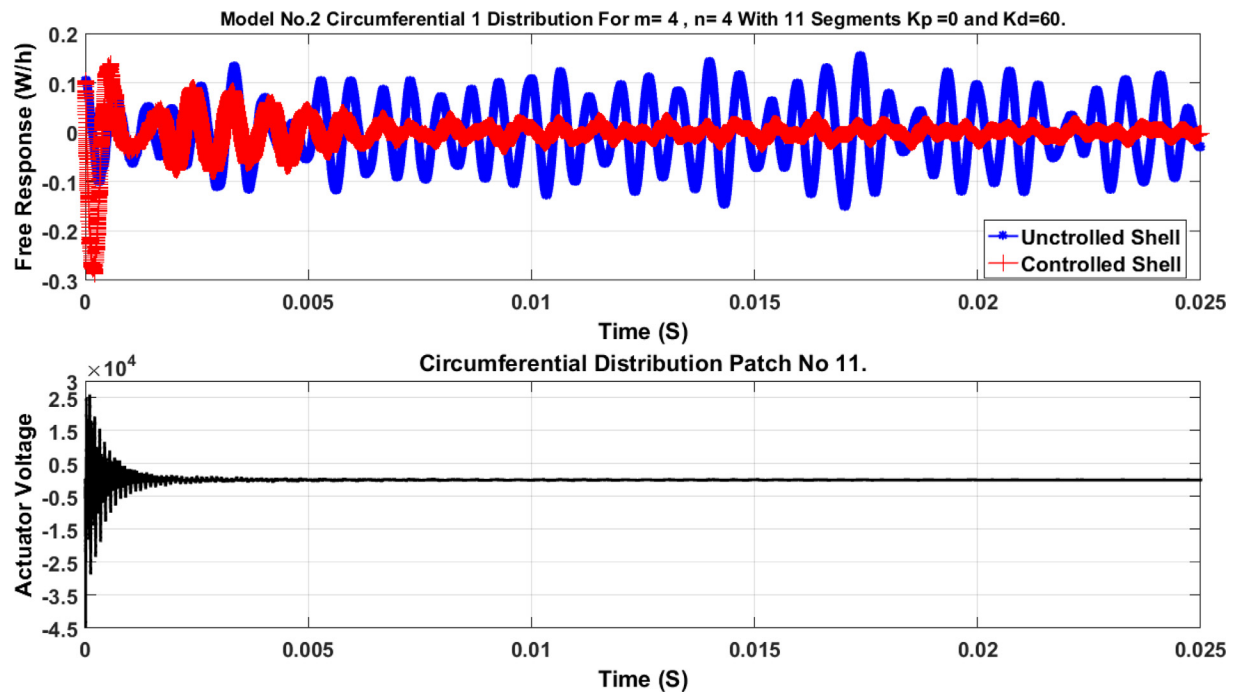


Fig. 9. Free vibration response of model No.2 in upper circumferential distribution with controller constants of $K_p = 0$ and $K_d = 60$. Maximum applied actuator voltage in patch No.11.

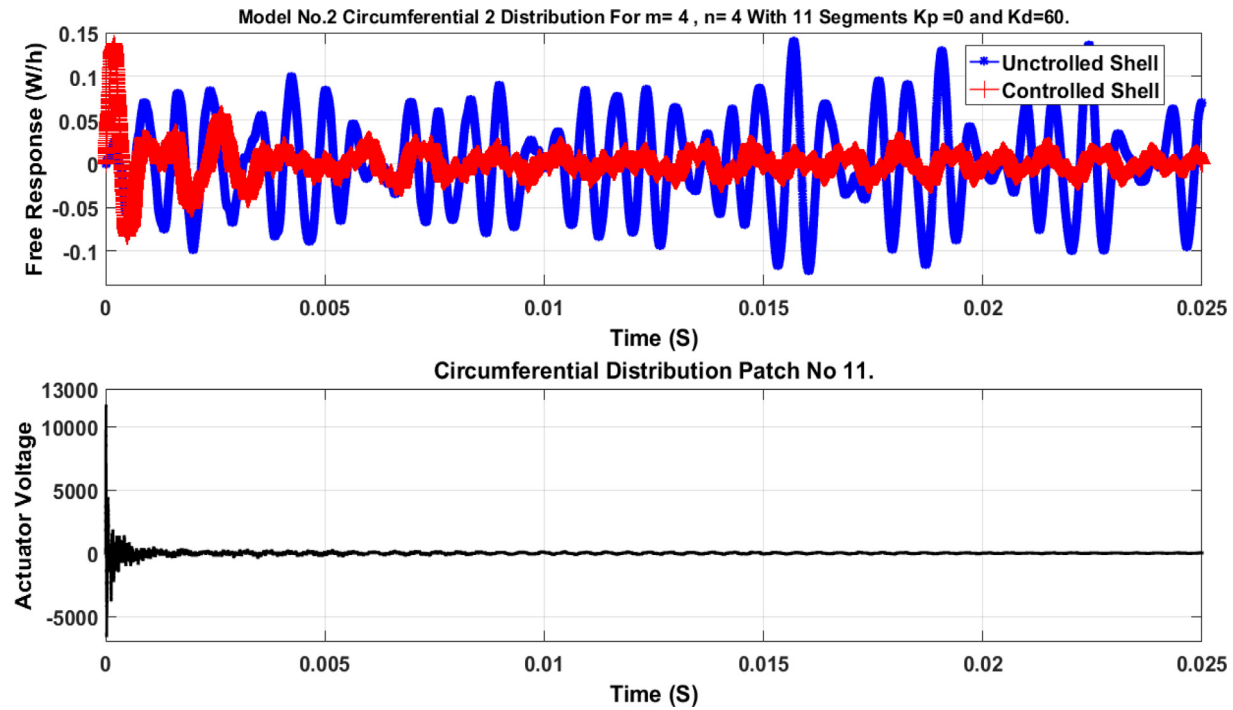


Fig. 10. Free vibration response of model No.2 in middle circumferential distribution with controller constants of $K_p = 0$ and $K_d = 60$. Maximum applied actuator voltage in patch No.11.

matically. Additionally, by comparing the presented results, the effect of piezoelectric layer distribution and controller types and constants can be evaluated. Whether circumferential distribution is more effective or longitudinal distribution and whether a proportional controller is more appealing or a derivative controller.

In overall, circumferential distribution affects the conical shell response dramatically. In contrast, longitudinal distribution effects

on conical shell frequency response is lower than circumferential distribution. Longitudinal distribution can reduce the frequency response amplitude in all of the excitation frequency range. However, circumferential distribution can reduce frequency response amplitude in higher excitation frequencies more effectively than lower excitation frequencies. In circumferential distributions, the controller can affect natural frequencies especially in higher excitation frequencies

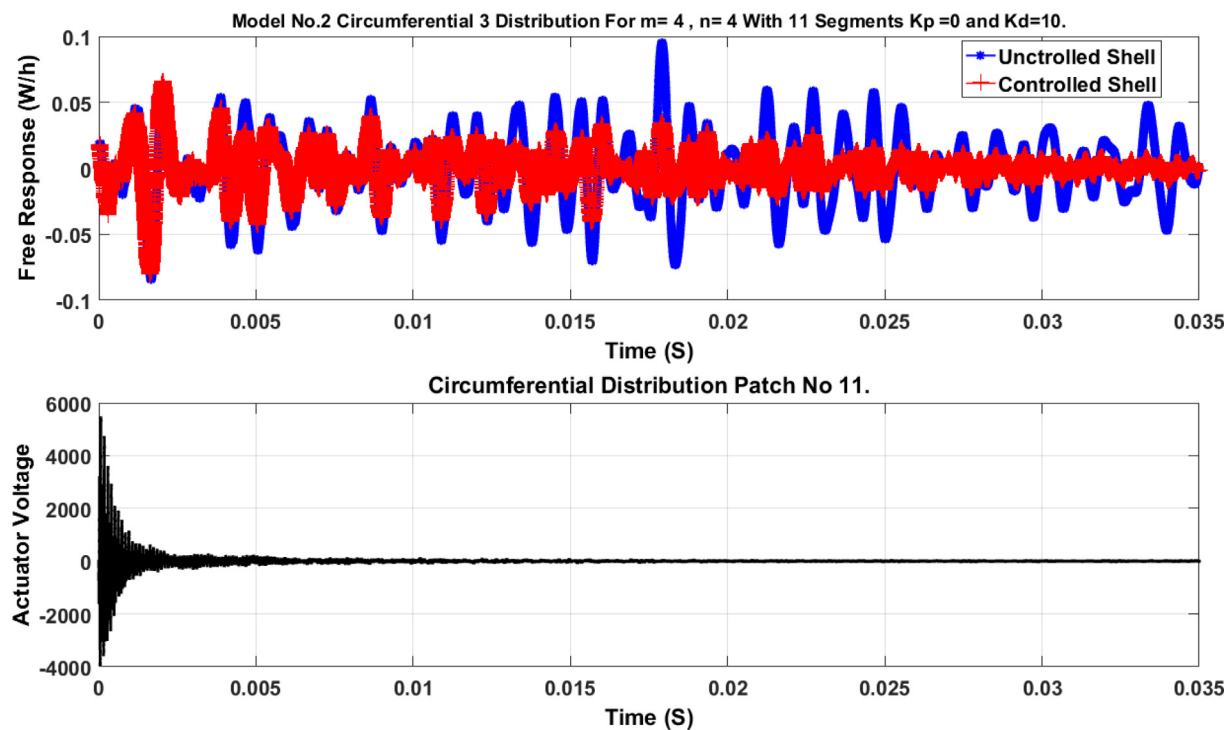


Fig. 11. Free vibration response of model No.2 in lower circumferential distribution with controller constants of $K_p = 0$ and $K_d = 10$. Maximum applied actuator voltage in patch No.11.

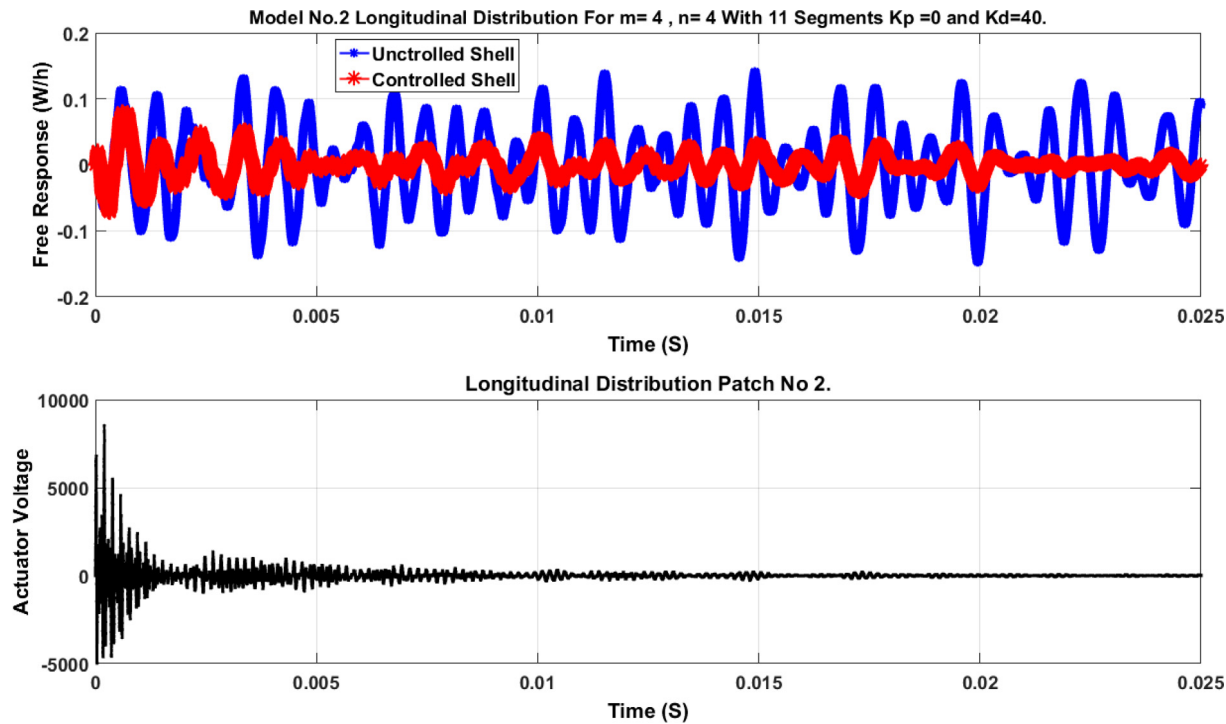


Fig. 12. Free vibration response of model No.2 in longitudinal distribution with controller constants of $K_p = 0$ and $K_d = 40$. Maximum applied actuator voltage in patch No.2.

and in lower circumferential piezoelectric distribution. While, in longitudinal distribution, the controller only decreases the response amplitude and it does not have much effect on the conical shell natural frequencies. In both considered models, the influence of the actuator/sensor layer at higher excitation frequencies is more explicit

than at lower excitation frequencies. The reason for this aspect is that changes in higher frequencies are more obvious than changes in lower frequencies, due to their greater amount.

In circumferential distribution, the derivative controller causes the response amplitude to decrease enormously. On the other hand, in

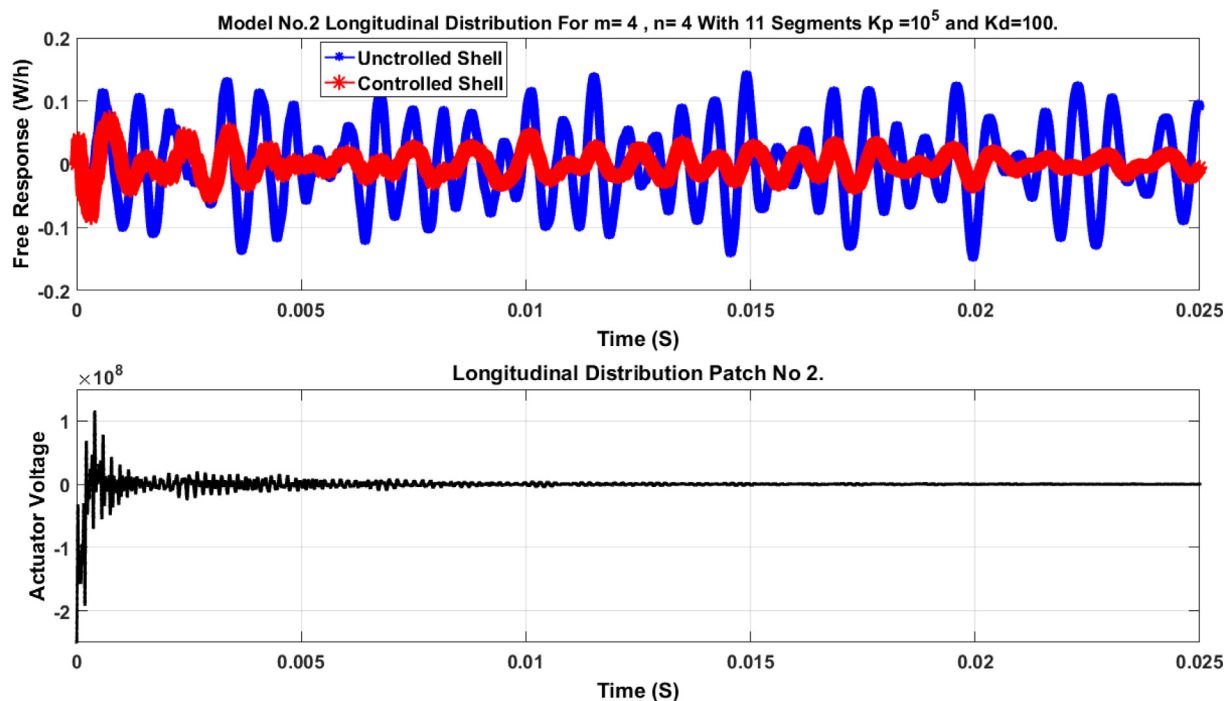


Fig. 13. Free vibration response of model No.2 in longitudinal distribution with controller constants of $K_p = 10^5$ and $K_d = 100$. Maximum applied actuator voltage in patch No.2.

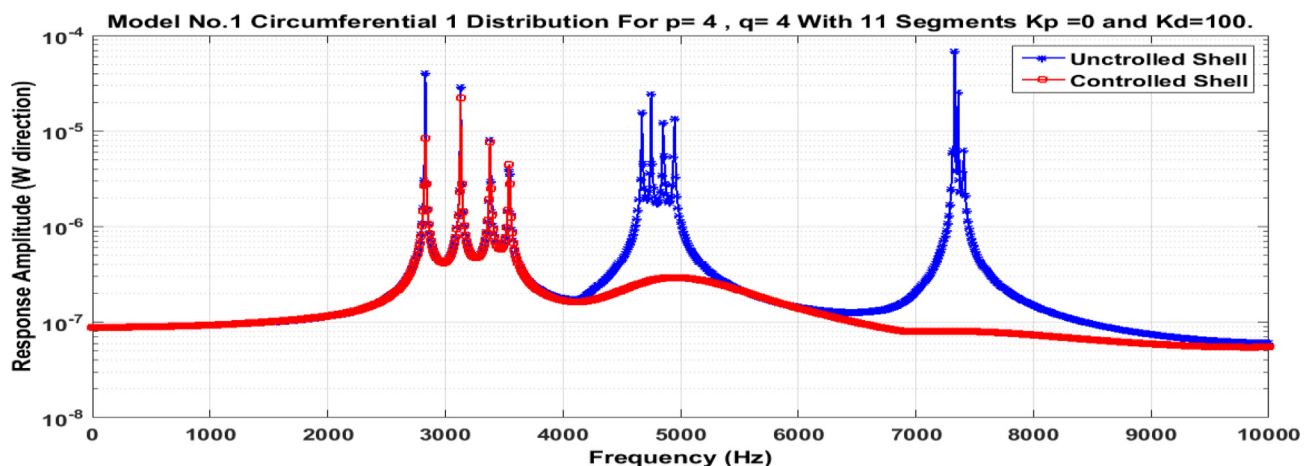


Fig. 14. Frequency response of conical shell model No.1 in uncontrolled condition in contrast to controlled condition with the upper circumferential distribution with controller constant of $K_p = 0$ and $K_d = 100$.

circumferential distribution the proportional controller causes the magnitude of natural frequencies to increase, especially in higher natural frequencies and in lower circumferential distribution.

Among all the considered circumferential distribution, the lower circumferential distribution has a major impact on the conical shell frequency response. The reason for this phenomenon is that the lower part of conical shells has a bigger radius and the structure is more flexible in that area rather than upperparts up of conical shell. Therefore, it is much easier to change the dynamic of the structure by forcing this part.

The derivative controller causes the system damping to increase and this can cause the frequency response amplitude to decrease. In circumferential distributions, the derivative controller can cause the response amplitude near natural frequencies to decrease highly, especially in higher excitation frequencies.

In circumferential distribution, if the sensor/actuator layer segments quantity was considered an even number, then in the frequency

response, the controlled and uncontrolled responses would become very similar and the effect of piezoelectric layers on the conical shell dynamics would decrease enormously. The reason for this is the decrease in observability and controllability due to the symmetricalness of distribution and structure.

10. Conclusion

In this study, conical shell control vibration with a sensor piezoelectric layer and an actuator piezoelectric layer which are connected by the proportional derivative controller is evaluated. For this purpose, at first electromechanical equations of motion of the considered system are extracted. Then the sensor output signal calculated and by considering a PD controller, actuator applied voltage computed. The electromechanical equations of motion based on strains are developed. Then the Galerkin method is used to solve the complicated equations.

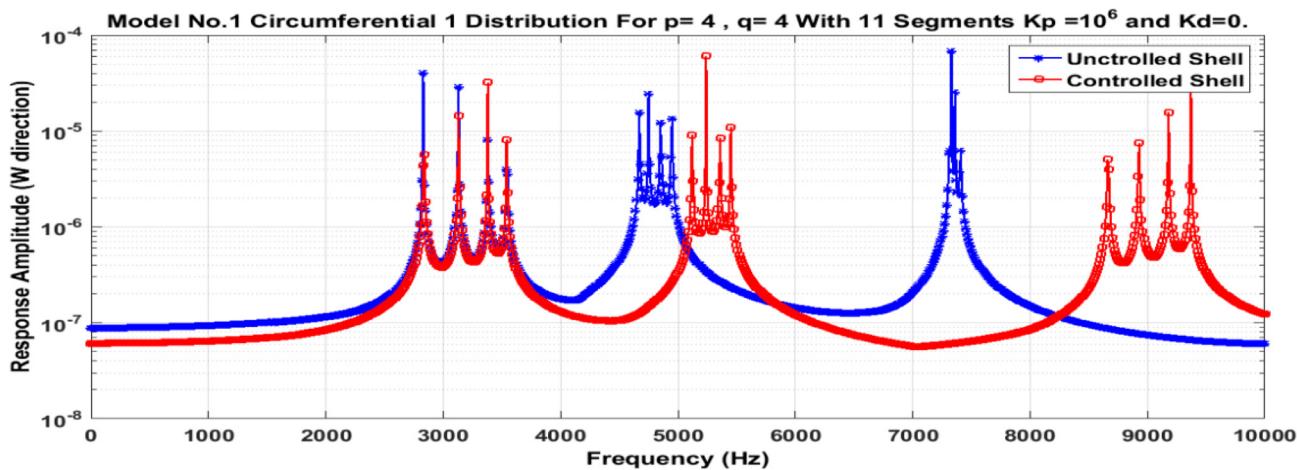


Fig. 15. Frequency response of conical shell model No.1 in uncontrolled condition in contrast to controlled condition with the upper circumferential distribution with controller constant of $K_p = 10^6$ and $K_d = 0$.

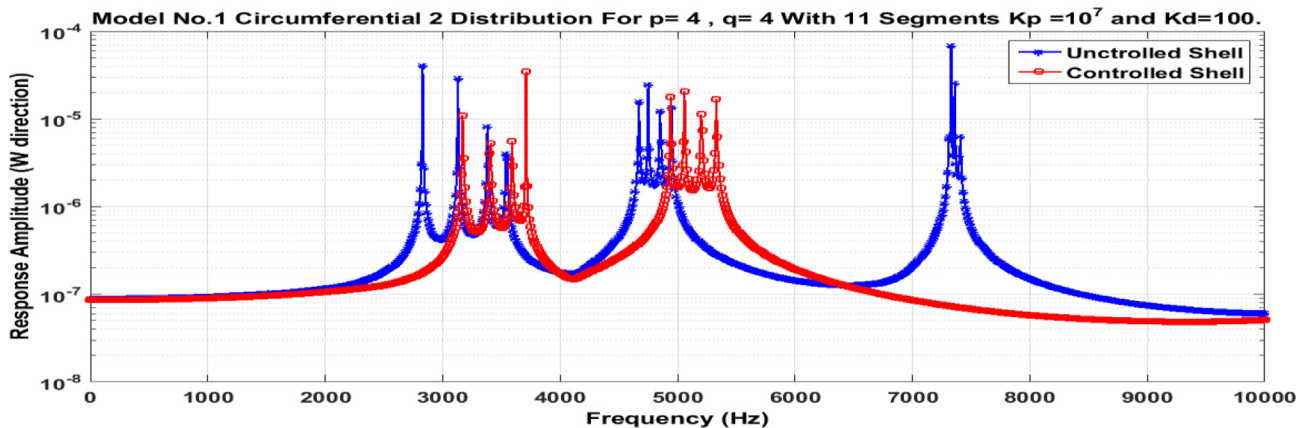


Fig. 16. Frequency response of conical shell model No.1 in uncontrolled condition in contrast to controlled condition with the middle circumferential distribution with controller constant of $K_p = 10^7$ and $K_d = 100$.

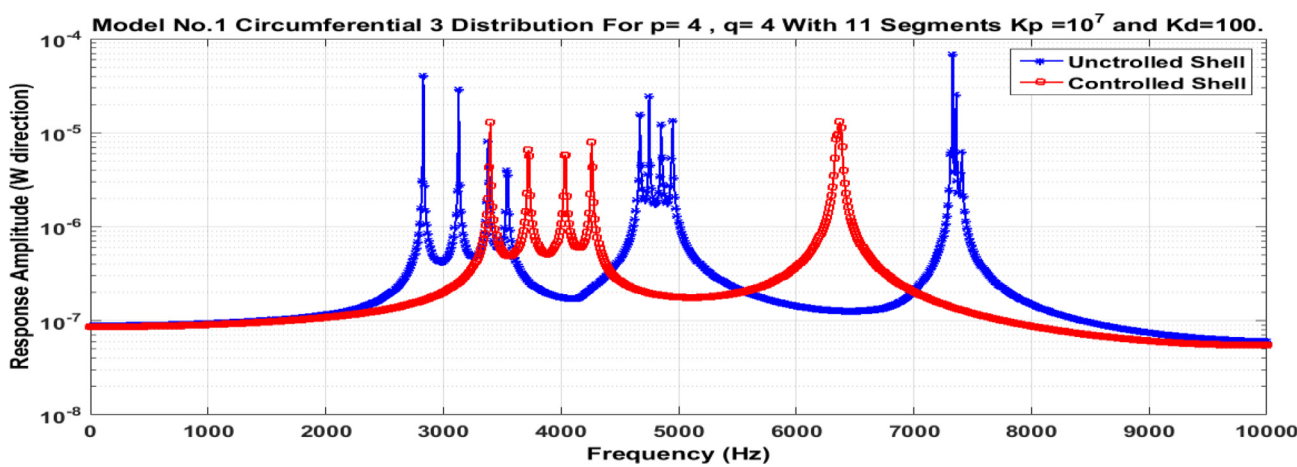


Fig. 17. Frequency response of conical shell model No.1 in uncontrolled condition in contrast to controlled condition with the lower circumferential distribution with controller constant of $K_p = 10^7$ and $K_d = 100$.

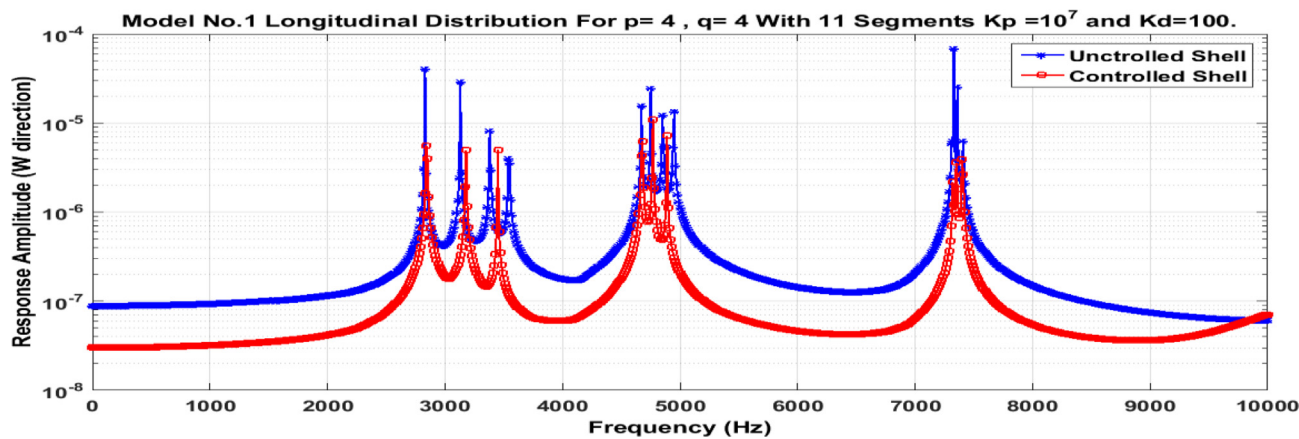


Fig. 18. Frequency response of model conical shell No.1 in uncontrolled condition in contrast to controlled condition with the longitudinal distribution with controller constant of $K_p = 10^7$ and $K_d = 100$.

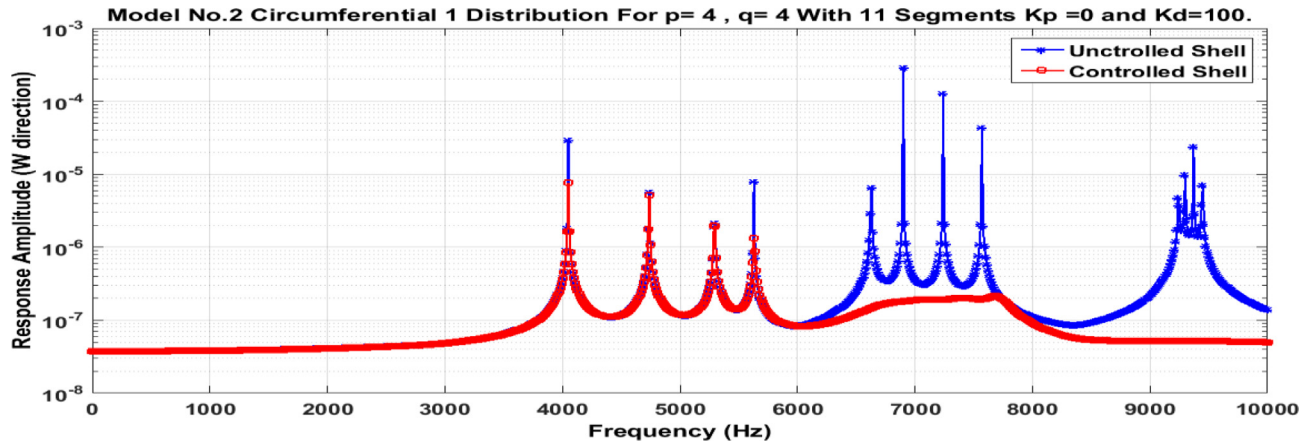


Fig. 19. Frequency response of conical shell model No.2 in uncontrolled condition in contrast to controlled condition with the upper circumferential distribution with controller constant of $K_p = 0$ and $K_d = 100$.

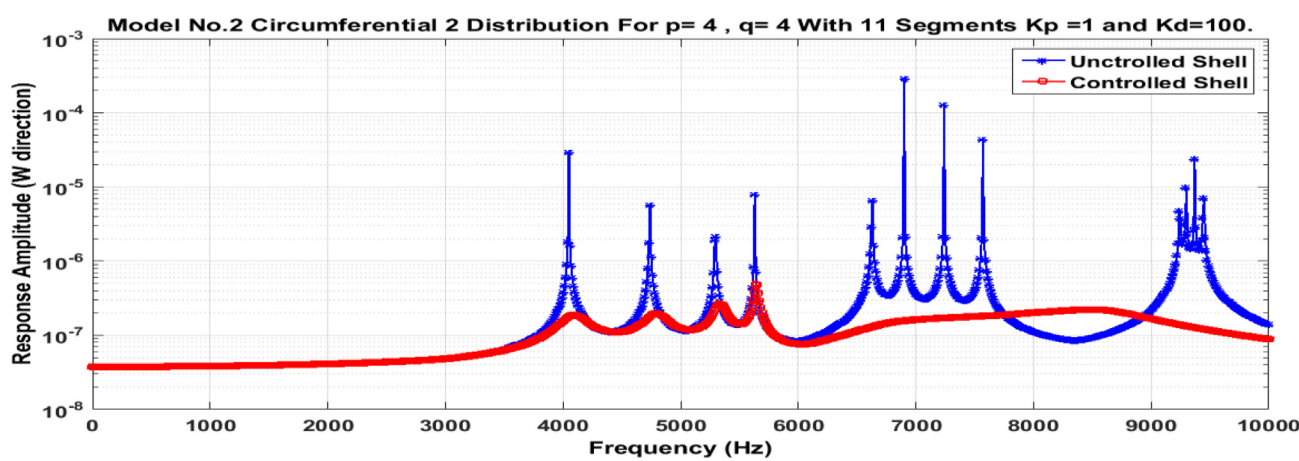


Fig. 20. Frequency response of conical shell model No.2 in uncontrolled condition in contrast to controlled condition with the middle circumferential distribution with controller constant of $K_p = 1$ and $K_d = 100$.

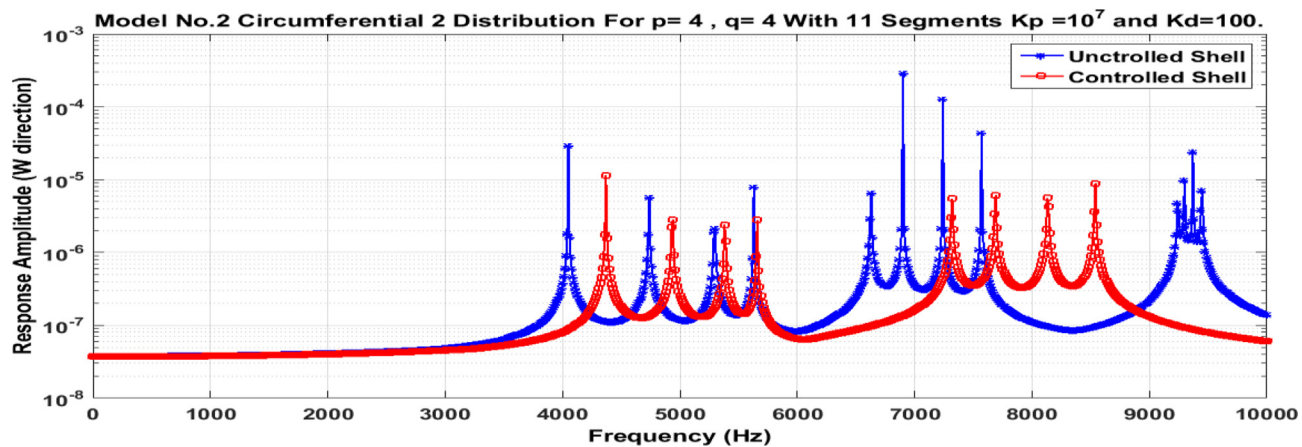


Fig. 21. Frequency response of conical shell model No.2 in uncontrolled condition in contrast to controlled condition with the middle circumferential distribution with controller constant of $K_p = 10^7$ and $K_d = 100$.

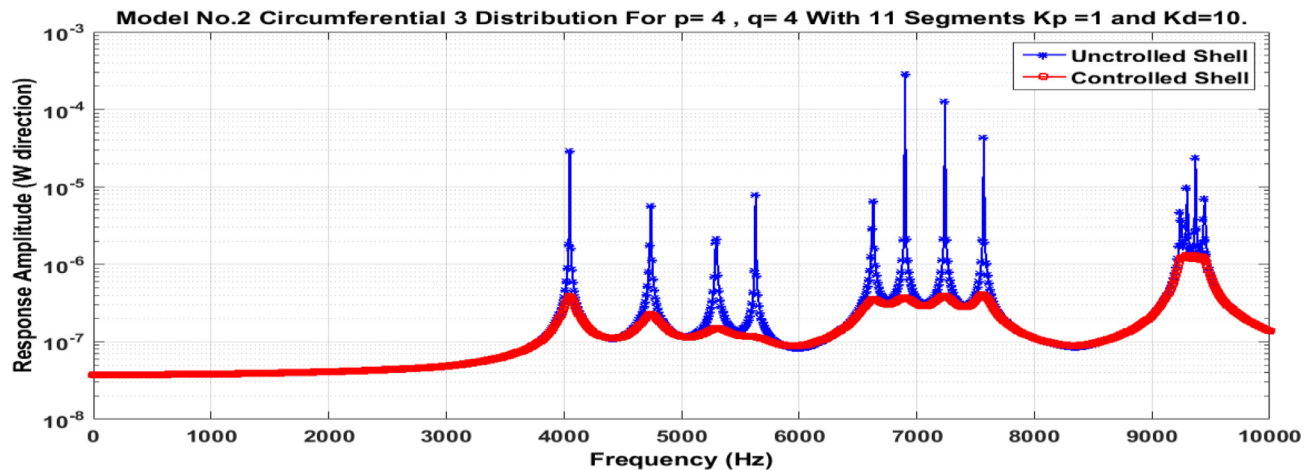


Fig. 22. Frequency response of conical shell model No.2 in uncontrolled condition in contrast to controlled condition with the lower circumferential distribution with controller constant of $K_p = 1$ and $K_d = 10$.

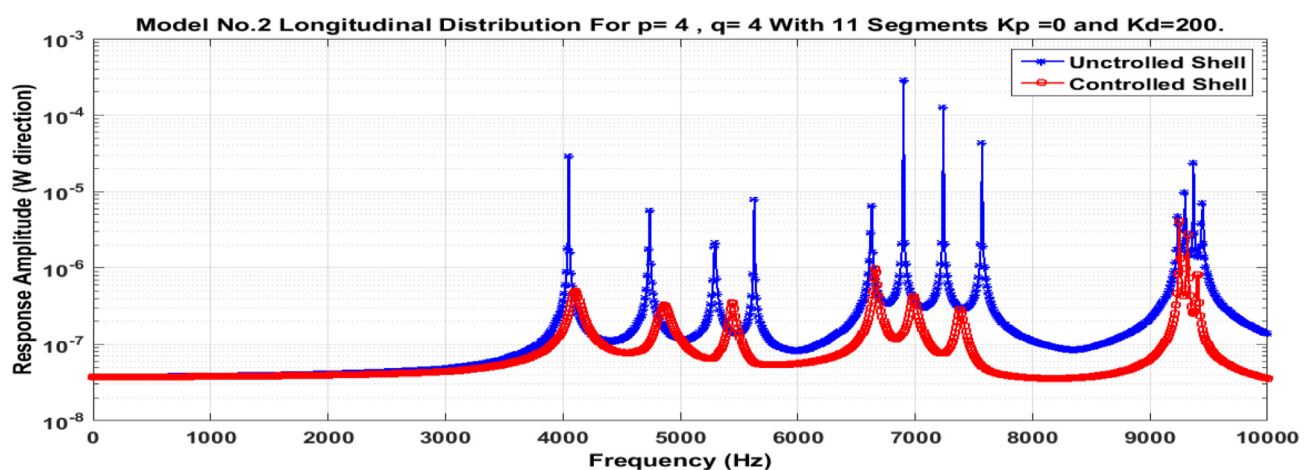


Fig. 23. Frequency response of conical shell model No.2 in uncontrolled condition in contrast to controlled condition with the longitudinal distribution with controller constant of $K_p = 0$ and $K_d = 200$.

Free vibration and frequency response of conical shells with various piezoelectric distribution are calculated. Sensor/actuator piezoelectric layer performance on vibration reduction is very desirable. In all of the displayed results, the effects of piezoelectric layers on the conical shells vibration level are definite and impeccable. The piezoelectric layer distribution and segmentation have a significant impact on its performance and especially the controller type has a consequential effect on conical shell dynamic. In circumferential distribution, the proportional controller causes natural frequencies to increase and the derivative controller causes the amplitude of response near natural frequencies to decrease enormously. These phenomena are apparent in higher excitation frequencies. In longitudinal distribution, controllers cannot affect the system dynamic near natural frequencies and cause the amplitude of response to decrease in other excitation frequencies. The lower circumferential distribution has an impeccable performance in contrast with other kinds of distributions.

CRediT authorship contribution statement

Rasa Jamshidi: Methodology, Software, Writing - original draft, Visualization, Investigation, Writing - review & editing. **A.A. Jafari:** Conceptualization, Supervision.

Declaration of Competing Interest

The authors declare that they have no known competing financial interests or personal relationships that could have appeared to influence the work reported in this paper.

Appendix A

Extracting electromechanical equation of motions of conical shells with piezoelectric layers

In this section, electromechanical equations of motion of conical shells with piezoelectric layer considering linear strains are extracted. For this purpose, a truncated conical shell with a piezoelectric sensor patch and a piezoelectric actuator patch with the same size and location is considered (Fig. 1). The linear strain displacement relationships are considered as demonstrated in Eq. (2). The total kinetic energy of considered system is the sum of conical shell kinetic energy and the actuator layer and the sensor layer kinetic energy (Eq. (A-1)).

$$\begin{aligned} T = & \frac{1}{2} \int_{x_1}^{x_2} \int_0^{2\pi} \int_{-\frac{h}{2}}^{\frac{h}{2}} \rho_m (\dot{u}^2 + \dot{v}^2 + \dot{w}^2) x \sin(\psi) dz d\theta dx + \frac{1}{2} \int_{x_1}^{x_2} \int_0^{2\pi} \\ & \times \int_{-\frac{h}{2}-h_s}^{-\frac{h}{2}} \rho_p (\dot{u}^2 + \dot{v}^2 + \dot{w}^2) x \sin(\psi) dz d\theta dx + \frac{1}{2} \int_{x_1}^{x_2} \int_0^{2\pi} \\ & \times \int_{\frac{h}{2}}^{\frac{h}{2}+h_a} \rho_p (\dot{u}^2 + \dot{v}^2 + \dot{w}^2) x \sin(\psi) dz d\theta dx \end{aligned} \quad (\text{A-1})$$

In Eq. (A-1), the first term is related to the conical shell kinetic energy and the second term is associated with the sensor layer kinetic energy and the third one is correlated with the actuator layer kinetic energy. Similarly, the overall potential energy of the system is the summation of conical shell potential energy, the actuator layer potential energy, and the sensor layer potential energy (Eq. A-2).

$$\begin{aligned} H = & \frac{1}{2} \int_{x_1}^{x_2} \int_0^{2\pi} \int_{-\frac{h}{2}}^{\frac{h}{2}} (\sigma_m \epsilon) x \sin(\psi) dz d\theta dx + \frac{1}{2} \int_{x_1}^{x_2} \int_0^{2\pi} \\ & \times \int_{-\frac{h}{2}-h_s}^{-\frac{h}{2}} (\sigma_p^s \epsilon) x \sin(\psi) dz d\theta dx + \frac{1}{2} \int_{x_1}^{x_2} \int_0^{2\pi} \\ & \times \int_{\frac{h}{2}}^{\frac{h}{2}+h_a} (\sigma_p^a \epsilon - D_p E) x \sin(\psi) dz d\theta dx \end{aligned} \quad (\text{A-2})$$

In the piezoelectric sensor layer, only the piezoelectric direct effect is considered and its converse effect is neglected. Therefore, in the piezoelectric sensor, the output voltage is used and only the mechanical potential energy of the layer is acknowledged in the overall system potential energy. Furthermore, in the piezoelectric actuator layer, its converse effect is considered and its direct effect is neglected. Therefore, the potential energy of the actuator is a summation of the mechanical and electrical energy of the piezoelectric layer.

In the conical shell and sensor layer, the relation between stress and strain is described based on the hook law.

$$\begin{bmatrix} \sigma_{xxm} \\ \sigma_{\theta\theta m} \\ \sigma_{x\theta m} \end{bmatrix} = \begin{bmatrix} Q_{11}^m & Q_{12}^m & 0 \\ Q_{12}^m & Q_{22}^m & 0 \\ 0 & 0 & Q_{33}^m \end{bmatrix} \begin{bmatrix} \epsilon_{xx} \\ \epsilon_{\theta\theta} \\ \epsilon_{x\theta} \end{bmatrix} \quad (\text{A-3})$$

$$\begin{bmatrix} \sigma_{xxp}^s \\ \sigma_{\theta\theta p}^s \\ \sigma_{x\theta p}^s \end{bmatrix} = \begin{bmatrix} Q_{11}^p & Q_{12}^p & 0 \\ Q_{12}^p & Q_{22}^p & 0 \\ 0 & 0 & Q_{33}^p \end{bmatrix} \begin{bmatrix} \epsilon_{xx} \\ \epsilon_{\theta\theta} \\ \epsilon_{x\theta} \end{bmatrix} \quad (\text{A-4})$$

The principal equations of piezoelectric for actuator layer are considered as:

$$\begin{bmatrix} \sigma_{xxp}^a \\ \sigma_{\theta\theta p}^a \\ \sigma_{x\theta p}^a \end{bmatrix} = \begin{bmatrix} Q_{11}^p & Q_{12}^p & 0 \\ Q_{12}^p & Q_{22}^p & 0 \\ 0 & 0 & Q_{33}^p \end{bmatrix} \begin{bmatrix} \epsilon_{xx} \\ \epsilon_{\theta\theta} \\ \epsilon_{x\theta} \end{bmatrix} - \begin{bmatrix} 0 & 0 & e_{31} \\ 0 & 0 & e_{32} \\ 0 & 0 & 0 \end{bmatrix} \begin{bmatrix} E_x \\ E_\theta \\ E_z \end{bmatrix} \quad (\text{A-5.a})$$

$$\begin{bmatrix} D_x \\ D_\theta \\ D_z \end{bmatrix} = \begin{bmatrix} 0 & 0 & 0 \\ 0 & 0 & 0 \\ e_{31} & e_{32} & 0 \end{bmatrix} \begin{bmatrix} \epsilon_{xx} \\ \epsilon_{\theta\theta} \\ \epsilon_{x\theta} \end{bmatrix} - \begin{bmatrix} \epsilon_{11} & 0 & 0 \\ 0 & \epsilon_{22} & 0 \\ 0 & 0 & \epsilon_{33} \end{bmatrix} \begin{bmatrix} E_x \\ E_\theta \\ E_z \end{bmatrix} \quad (\text{A-5.b})$$

In this study, only the transverse electric field (E_z) is considered and the surface electric fields (E_x, E_θ) are neglected. Thereby, the actuator layer stresses and electrical displacement can be calculated from Eqs. (A-6) and (A-7).

$$\sigma_{xxp}^a = \frac{E_p}{1 - \nu_p^2} (\epsilon_{xx} + \nu_p \epsilon_{\theta\theta}) - e_{31} E_z = \sigma_{xxmp}^a - e_{31} E_z \quad (\text{A-6.a})$$

$$\sigma_{\theta\theta p}^a = \frac{E_p}{1 - \nu_p^2} (\epsilon_{\theta\theta} + \nu_p \epsilon_{xx}) - e_{32} E_z = \sigma_{\theta\theta mp}^a - e_{32} E_z \quad (\text{A-6.b})$$

$$\sigma_{x\theta p}^a = \frac{E_p}{2(1 + \nu_p)} \epsilon_{x\theta} = \sigma_{x\theta mp}^a \quad (\text{A-6.c})$$

$$D_x = 0, D_\theta = 0 \quad (\text{A-7.a})$$

$$D_z = e_{31} \epsilon_{xx} + e_{32} \epsilon_{\theta\theta} + \epsilon_{33} E_z \quad (\text{A-7.b})$$

Considering Eq. (A-7), the Eq. (A-2) can be developed as:

$$\begin{aligned} H = & \frac{1}{2} \int_{x_1}^{x_2} \int_0^{2\pi} \int_{-\frac{h}{2}}^{\frac{h}{2}} (\sigma_{xxm}^m \epsilon_{xx} + \sigma_{\theta\theta m}^m \epsilon_{\theta\theta} + \sigma_{x\theta m}^m \epsilon_{x\theta}) x \sin(\psi) dz d\theta dx \\ & + \frac{1}{2} \int_{x_1}^{x_2} \int_0^{2\pi} \int_{-\frac{h}{2}-h_s}^{-\frac{h}{2}} (\sigma_{xxp}^s \epsilon_{xx} + \sigma_{\theta\theta p}^s \epsilon_{\theta\theta} + \sigma_{x\theta p}^s \epsilon_{x\theta}) x \sin(\psi) dz d\theta dx \\ & + \frac{1}{2} \int_{x_1}^{x_2} \int_0^{2\pi} \int_{\frac{h}{2}}^{\frac{h}{2}+h_a} (\sigma_{xxp}^a \epsilon_{xx} + \sigma_{\theta\theta p}^a \epsilon_{\theta\theta} + \sigma_{x\theta p}^a \epsilon_{x\theta}) x \sin(\psi) dz d\theta dx \\ & - e_{32} E_z \epsilon_{\theta\theta} - e_{33} E_z^2 \end{aligned} \quad (\text{A-8})$$

Arranging Eq. (A-8) leads to:

$$\begin{aligned}
H = & \frac{1}{2} \int_{x_1}^{x_2} \int_0^{2\pi} \int_{-\frac{h}{2}}^{\frac{h}{2}} (\sigma_{xx}^m \varepsilon_{xx} + \sigma_{\theta\theta}^m \varepsilon_{\theta\theta} + \sigma_{x\theta}^m \varepsilon_{x\theta}) x \sin(\psi) dz d\theta dx + \frac{1}{2} \int_{x_1}^{x_2} \\
& \times \int_0^{2\pi} \int_{-\frac{h}{2}-h_s}^{\frac{h}{2}} (\sigma_{xxp}^s \varepsilon_{xx} + \sigma_{\theta\theta p}^s \varepsilon_{\theta\theta} + \sigma_{x\theta p}^s \varepsilon_{x\theta}) x \sin(\psi) dz d\theta dx + \frac{1}{2} \int_{x_1}^{x_2} \\
& \times \int_0^{2\pi} \int_{\frac{h}{2}}^{\frac{h}{2}+h_a} ((\sigma_{xxmp}^a - e_{31}E_z) \varepsilon_{xx} + (\sigma_{\theta\theta mp}^a - e_{32}E_z) \varepsilon_{\theta\theta} + \sigma_{x\theta mp}^a \varepsilon_{x\theta} \\
& - (e_{31}\varepsilon_{xx}E_z + e_{32}\varepsilon_{\theta\theta}E_z + e_{33}E_z^2)) x \sin(\psi) dz d\theta dx
\end{aligned} \quad (A9)$$

Considering Eq. (A-9), the variation of total potential energy of the system is extracted.

$$\begin{aligned}
\delta H = & \frac{1}{2} \int_{x_1}^{x_2} \int_0^{2\pi} \int_{-\frac{h}{2}}^{\frac{h}{2}} (\sigma_{xx}^m \delta \varepsilon_{xx} + \sigma_{\theta\theta}^m \delta \varepsilon_{\theta\theta} + \sigma_{x\theta}^m \delta \varepsilon_{x\theta}) x \sin(\psi) dz d\theta dx + \frac{1}{2} \int_{x_1}^{x_2} \\
& \times \int_0^{2\pi} \int_{-\frac{h}{2}-h_s}^{\frac{h}{2}} (\sigma_{xxp}^s \delta \varepsilon_{xx} + \sigma_{\theta\theta p}^s \delta \varepsilon_{\theta\theta} + \sigma_{x\theta p}^s \delta \varepsilon_{x\theta}) x \sin(\psi) dz d\theta dx + \frac{1}{2} \\
& \times \int_{x_1}^{x_2} \int_0^{2\pi} \\
& \times \int_{\frac{h}{2}}^{\frac{h}{2}+h_a} ((\sigma_{xxmp}^a - e_{31}E_z) \delta \varepsilon_{xx} + (\sigma_{\theta\theta mp}^a - e_{32}E_z) \delta \varepsilon_{\theta\theta} + \sigma_{x\theta mp}^a \delta \varepsilon_{x\theta} \\
& - (e_{31}\varepsilon_{xx} + e_{32}\varepsilon_{\theta\theta} + e_{33}E_z) \delta E_z) x \sin(\psi) dz d\theta dx
\end{aligned} \quad (A10)$$

For calculating variation of total potential energy, at first variation of conical shell strains should be computed. For this purpose, the variations of conical shell strains are extracted from Eq. (1).

$$\delta \varepsilon_{xx} = \delta \varepsilon_{xx}^0 + z \delta k_{xx} \quad (A-11.a)$$

$$\delta \varepsilon_{\theta\theta} = \delta \varepsilon_{\theta\theta}^0 + z \delta k_{\theta\theta} \quad (A-11.b)$$

$$\delta \varepsilon_{x\theta} = \delta \varepsilon_{x\theta}^0 + z \delta k_{x\theta} \quad (A-11.c)$$

It is mentioned that the transverse electric field equation is considered as below:

$$E_z = -\frac{\partial \varphi}{\partial z} \quad (A12)$$

The mechanical membrane forces and bending moments of conical shell are considered as:

$$N_{xx}^m = \int_{-\frac{h}{2}}^{\frac{h}{2}} \sigma_{xx}^m dz \quad (A-13.a)$$

$$N_{\theta\theta}^m = \int_{-\frac{h}{2}}^{\frac{h}{2}} \sigma_{\theta\theta}^m dz \quad (A-13.b)$$

$$N_{x\theta}^m = \int_{-\frac{h}{2}}^{\frac{h}{2}} \sigma_{x\theta}^m dz \quad (A-13.c)$$

$$M_{xx}^m = \int_{-\frac{h}{2}}^{\frac{h}{2}} \sigma_{xx}^m z dz \quad (A-13.d)$$

$$M_{\theta\theta}^m = \int_{-\frac{h}{2}}^{\frac{h}{2}} \sigma_{\theta\theta}^m z dz \quad (A-13.e)$$

$$M_{x\theta}^m = \int_{-\frac{h}{2}}^{\frac{h}{2}} \sigma_{x\theta}^m z dz \quad (A-13.f)$$

Similarly, mechanical membrane forces and bending moments of the piezoelectric sensor layer is regarded as:

$$N_{xx}^{ms} = \int_{-\frac{h}{2}-h_s}^{-\frac{h}{2}} \sigma_{xxp}^s dz \quad (A-14.a)$$

$$N_{\theta\theta}^{ms} = \int_{-\frac{h}{2}-h_s}^{-\frac{h}{2}} \sigma_{\theta\theta p}^s dz \quad (A-14.b)$$

$$N_{x\theta}^{ms} = \int_{-\frac{h}{2}-h_s}^{-\frac{h}{2}} \sigma_{x\theta p}^s dz \quad (A-14.c)$$

$$M_{xx}^{ms} = \int_{-\frac{h}{2}-h_s}^{-\frac{h}{2}} \sigma_{xxp}^s z dz \quad (A-14.d)$$

$$M_{\theta\theta}^{ms} = \int_{-\frac{h}{2}-h_s}^{-\frac{h}{2}} \sigma_{\theta\theta p}^s z dz \quad (A-14.e)$$

$$M_{x\theta}^{ms} = \int_{-\frac{h}{2}-h_s}^{-\frac{h}{2}} \sigma_{x\theta p}^s z dz \quad (A-14.f)$$

Also, mechanical membrane forces and bending moments of the actuator layer is granted as:

$$N_{xx}^{ma} = \int_{\frac{h}{2}}^{\frac{h}{2}+h_a} \sigma_{xxmp}^a dz \quad (A-15.a)$$

$$N_{\theta\theta}^{ma} = \int_{\frac{h}{2}}^{\frac{h}{2}+h_a} \sigma_{\theta\theta mp}^a dz \quad (A-15.b)$$

$$N_{x\theta}^{ma} = \int_{\frac{h}{2}}^{\frac{h}{2}+h_a} \sigma_{x\theta mp}^a dz \quad (A-15.c)$$

$$M_{xx}^{ma} = \int_{\frac{h}{2}}^{\frac{h}{2}+h_a} \sigma_{xxmp}^a z dz \quad (A-15.d)$$

$$M_{\theta\theta}^{ma} = \int_{\frac{h}{2}}^{\frac{h}{2}+h_a} \sigma_{\theta\theta mp}^a z dz \quad (A-15.e)$$

$$M_{x\theta}^{ma} = \int_{\frac{h}{2}}^{\frac{h}{2}+h_a} \sigma_{x\theta mp}^a z dz \quad (A-15.f)$$

Finally, electrical membrane forces and bending moments of actuator layer is considered as below.

$$N_{xx}^e = \int_{\frac{h}{2}}^{\frac{h}{2}+h_a} e_{31}E_z dz \quad (A-16.a)$$

$$N_{\theta\theta}^e = \int_{\frac{h}{2}}^{\frac{h}{2}+h_a} e_{32}E_z dz \quad (A-16.b)$$

$$N_{x\theta}^e = 0 \quad (A-16.c)$$

$$M_{xx}^e = \int_{\frac{h}{2}}^{\frac{h}{2}+h_a} e_{31}E_z z dz \quad (A-16.d)$$

$$M_{\theta\theta}^e = \int_{\frac{h}{2}}^{\frac{h}{2}+h_a} e_{32}E_z z dz \quad (A-16.e)$$

$$M_{x\theta}^e = 0 \quad (A-16.f)$$

The Eq. (A-10) is rewritten with considering Eqs. (A-11) to (A-16).

$$\begin{aligned}
\delta H = & \frac{1}{2} \int_{x_1}^{x_2} \left[-\frac{\partial}{\partial x} (N_{xx}^m + N_{xx}^{ms} + N_{xx}^{ma} - N_{xx}^e) x \sin(\psi) \right] d\theta dx \\
& \times \int_0^{2\pi} (N_{xx}^m \delta \epsilon_{xx}^0 + M_{xx}^m \delta k_x + N_{\theta\theta}^m \delta \epsilon_{\theta\theta}^0 + M_{\theta\theta}^m \delta k_\theta + N_{x\theta}^m \delta \epsilon_{x\theta}^0 + M_{x\theta}^m \delta k_{x\theta}) x \sin(\psi) d\theta dx \\
& + \frac{1}{2} \int_{x_1}^{x_2} \left[-\frac{\partial}{\partial x} (N_{xx}^{ms} + M_{xx}^{ms} \delta k_x + N_{\theta\theta}^{ms} \delta \epsilon_{\theta\theta}^0 + M_{\theta\theta}^{ms} \delta k_\theta + N_{x\theta}^{ms} \delta \epsilon_{x\theta}^0 + M_{x\theta}^{ms} \delta k_{x\theta}) x \sin(\psi) \right] dz d\theta dx \\
& \times \int_0^{2\pi} (N_{xx}^{ms} \delta \epsilon_{xx}^0 + M_{xx}^{ms} \delta k_x + N_{\theta\theta}^{ms} \delta \epsilon_{\theta\theta}^0 + M_{\theta\theta}^{ms} \delta k_\theta + N_{x\theta}^{ms} \delta \epsilon_{x\theta}^0 + M_{x\theta}^{ms} \delta k_{x\theta}) x \sin(\psi) dz d\theta dx \\
& + \frac{1}{2} \int_{x_1}^{x_2} \left[-\frac{\partial}{\partial x} (N_{xx}^{ma} + M_{xx}^{ma} \delta k_x + N_{\theta\theta}^{ma} \delta \epsilon_{\theta\theta}^0 + M_{\theta\theta}^{ma} \delta k_\theta + N_{x\theta}^{ma} \delta \epsilon_{x\theta}^0 + M_{x\theta}^{ma} \delta k_{x\theta}) x \sin(\psi) \right] dz d\theta dx \\
& - \frac{1}{2} \int_{x_1}^{x_2} \int_0^{2\pi} (N_{xx}^e \delta \epsilon_{xx}^0 + M_{xx}^e \delta k_x + N_{\theta\theta}^e \delta \epsilon_{\theta\theta}^0 + M_{\theta\theta}^e \delta k_\theta) x \sin(\psi) dz d\theta dx - \frac{1}{2} \\
& \times \int_{x_1}^{x_2} \int_0^{2\pi} (e_{31} \epsilon_{xx} + e_{32} \epsilon_{\theta\theta} + e_{33} E_z) \delta E_z x \sin(\psi) dz d\theta dx
\end{aligned} \tag{A-17}$$

The Eq. (A-18) is derived based on Eq. (A-17) and regarding strain-displacement equations.

$$\begin{aligned}
\delta H = & \frac{1}{2} \int_{x_1}^{x_2} \int_0^{2\pi} \left[(N_{xx}^m + N_{xx}^{ms} + N_{xx}^{ma} - N_{xx}^e) \frac{\partial(\delta u)}{\partial x} \right. \\
& - (M_{xx}^m + M_{xx}^{ms} + M_{xx}^{ma} - M_{xx}^e) \frac{\partial^2(\delta w)}{\partial x^2} + (N_{\theta\theta}^m + N_{\theta\theta}^{ms} + N_{\theta\theta}^{ma} - N_{\theta\theta}^e) \left(\frac{\delta u}{x} + \frac{\delta w}{x \tan(\psi)} \right) \\
& + (N_{\theta\theta}^m + N_{\theta\theta}^{ms} + N_{\theta\theta}^{ma} - N_{\theta\theta}^e) \left(\frac{1}{x \sin(\psi)} \right) \frac{\partial(\delta v)}{\partial \theta} \\
& + (M_{\theta\theta}^m + M_{\theta\theta}^{ms} + M_{\theta\theta}^{ma} - M_{\theta\theta}^e) \left(\frac{\cos(\psi)}{(x \sin(\psi))^2} \frac{\partial(\delta v)}{\partial \theta} - \frac{1}{(x \sin(\psi))^2} \frac{\partial^2(\delta w)}{\partial \theta^2} - \frac{1}{x} \frac{\partial(\delta w)}{\partial x} \right) \\
& + (N_{x\theta}^m + N_{x\theta}^{ms} + N_{x\theta}^{ma}) \left(\frac{1}{(x \sin(\psi))} \frac{\partial(\delta u)}{\partial x} - \frac{\delta v}{x} + \frac{\partial(\delta v)}{\partial x} \right) \\
& + (M_{x\theta}^m + M_{x\theta}^{ms} + M_{x\theta}^{ma}) \left(\frac{1}{(x \tan(\psi))} \frac{\partial(\delta v)}{\partial x} - \frac{2 \delta v}{x^2 \tan(\psi)} - \frac{2}{x \sin(\psi)} \frac{\partial^2(\delta w)}{\partial x \partial \theta} + \frac{2}{x^2 \sin(\psi)} \frac{\partial(\delta w)}{\partial \theta} \right) \\
& \pm (e_{31} \epsilon_{xx} + e_{32} \epsilon_{\theta\theta} + e_{33} E_z) \frac{\partial(\delta \varphi)}{\partial z} x \sin(\psi) d\theta dx
\end{aligned} \tag{A-18}$$

For extracting equations based on displacement variation in three directions and voltage variation, the divergence equation is used. After implementing divergence equation on Eq. (A-18), the equation leads to:

$$\begin{aligned}
\delta H = & \frac{1}{2} \int_{x_1}^{x_2} \int_0^{2\pi} \left[-\frac{\partial}{\partial x} ((N_{xx}^m + N_{xx}^{ms} + N_{xx}^{ma} - N_{xx}^e) x \sin(\psi)) \delta u \right. \\
& - \frac{\partial^2}{\partial x^2} ((M_{xx}^m + M_{xx}^{ms} + M_{xx}^{ma} - M_{xx}^e) x \sin(\psi)) \delta w \\
& + (N_{\theta\theta}^m + N_{\theta\theta}^{ms} + N_{\theta\theta}^{ma} - N_{\theta\theta}^e) (\sin(\psi) \delta u + \cos(\psi) \delta w) \\
& - \frac{\partial}{\partial \theta} (N_{\theta\theta}^m + N_{\theta\theta}^{ms} + N_{\theta\theta}^{ma} - N_{\theta\theta}^e) \delta v \\
& - \frac{\partial}{\partial \theta} \left((M_{\theta\theta}^m + M_{\theta\theta}^{ms} + M_{\theta\theta}^{ma} - M_{\theta\theta}^e) \frac{\cos(\psi)}{x \sin(\psi)} \right) \delta v \\
& - \frac{\partial^2}{\partial \theta^2} \left((M_{\theta\theta}^m + M_{\theta\theta}^{ms} + M_{\theta\theta}^{ma} - M_{\theta\theta}^e) \frac{1}{x \sin(\psi)} \right) \delta w \\
& + \frac{\partial}{\partial x} ((M_{\theta\theta}^m + M_{\theta\theta}^{ms} + M_{\theta\theta}^{ma} - M_{\theta\theta}^e) \sin(\psi)) \delta w \\
& - \frac{\partial}{\partial x} (N_{x\theta}^m + N_{x\theta}^{ms} + N_{x\theta}^{ma}) \delta u - (N_{x\theta}^m + N_{x\theta}^{ms} + N_{x\theta}^{ma}) \sin(\psi) \delta v \\
& - \frac{\partial}{\partial x} ((N_{x\theta}^m + N_{x\theta}^{ms} + N_{x\theta}^{ma}) x \sin(\psi)) \delta v \\
& - \frac{\partial}{\partial x} ((M_{x\theta}^m + M_{x\theta}^{ms} + M_{x\theta}^{ma}) \cos(\psi)) \delta v \\
& - \frac{2 \cos(\psi)}{x} (M_{x\theta}^m + M_{x\theta}^{ms} + M_{x\theta}^{ma}) \delta v - 2 \\
& \times \frac{\partial^2}{\partial x \partial \theta} (M_{x\theta}^m + M_{x\theta}^{ms} + M_{x\theta}^{ma}) \delta w - \frac{2}{x} \frac{\partial}{\partial \theta} (M_{x\theta}^m + M_{x\theta}^{ms} + M_{x\theta}^{ma}) \delta w \\
& - \frac{\partial}{\partial z} ((e_{31} \epsilon_{xx} + e_{32} \epsilon_{\theta\theta} + e_{33} E_z) x \sin(\psi)) \delta \varphi d\theta dx
\end{aligned} \tag{A-19}$$

Parameters with the same variation factor are arranged together and obtained equation is presented in Eq. (A-20).

$$\begin{aligned}
\delta H = & \frac{1}{2} \int_{x_1}^{x_2} \int_0^{2\pi} \left[\left[-\frac{\partial}{\partial x} (N_{xx}^m + N_{xx}^{ms} + N_{xx}^{ma} - N_{xx}^e) x \sin(\psi) \right. \right. \\
& - (N_{xx}^m + N_{xx}^{ms} + N_{xx}^{ma} - N_{xx}^e) \sin(\psi) + (N_{\theta\theta}^m + N_{\theta\theta}^{ms} + N_{\theta\theta}^{ma} - N_{\theta\theta}^e) \sin(\psi) \\
& - \frac{\partial}{\partial x} (N_{\theta\theta}^m + N_{\theta\theta}^{ms} + N_{\theta\theta}^{ma}) \sin(\psi) - \frac{\partial}{\partial x} (N_{x\theta}^m + N_{x\theta}^{ms} + N_{x\theta}^{ma}) x \sin(\psi) \\
& - 2 (N_{x\theta}^m + N_{x\theta}^{ms} + N_{x\theta}^{ma}) \sin(\psi) - \frac{\partial}{\partial x} (M_{x\theta}^m + M_{x\theta}^{ms} + M_{x\theta}^{ma}) \cos(\psi) - \frac{2 \cos(\psi)}{x} (M_{x\theta}^m + M_{x\theta}^{ms} + M_{x\theta}^{ma}) \\
& - 2 \frac{\partial}{\partial x} (M_{x\theta}^m + M_{x\theta}^{ms} + M_{x\theta}^{ma} - M_{x\theta}^e) \sin(\psi) \\
& + (N_{\theta\theta}^m + N_{\theta\theta}^{ms} + N_{\theta\theta}^{ma} - N_{\theta\theta}^e) \cos(\psi) \\
& - \frac{\partial^2}{\partial \theta^2} (M_{\theta\theta}^m + M_{\theta\theta}^{ms} + M_{\theta\theta}^{ma} - M_{\theta\theta}^e) \frac{1}{x \sin(\psi)} \\
& + \frac{\partial}{\partial x} (M_{\theta\theta}^m + M_{\theta\theta}^{ms} + M_{\theta\theta}^{ma} - M_{\theta\theta}^e) \sin(\psi) - 2 \\
& \times \frac{\partial^2}{\partial x \partial \theta} (M_{\theta\theta}^m + M_{\theta\theta}^{ms} + M_{\theta\theta}^{ma} - M_{\theta\theta}^e) - \frac{2}{x} \frac{\partial}{\partial \theta} (M_{\theta\theta}^m + M_{\theta\theta}^{ms} + M_{\theta\theta}^{ma}) \\
& \left. \left. + \left[-\frac{\partial}{\partial z} ((e_{31} \epsilon_{xx} + e_{32} \epsilon_{\theta\theta} + e_{33} E_z) x \sin(\psi)) \right] \delta \varphi \right] d\theta dx \right]
\end{aligned} \tag{A-20}$$

As it is shown, all of the terms are arranged based on δu , δv , δw and $\delta \varphi$. These terms will be presented in the final electromechanical equations of the conical shell with the piezoelectric sensor and actuator layer. In the next step, the variation of conical shell kinetic energy with actuator and sensor layer is extracted. Considering Eq. (A-1), the variation of kinetic energy is derived.

$$\begin{aligned}
\delta T = & -\frac{1}{2} \int_{x_1}^{x_2} \int_0^{2\pi} \int_{-\frac{h}{2}}^{\frac{h}{2}} \rho_m (\ddot{u} \delta u + \ddot{v} \delta v + \ddot{w} \delta w) x \sin(\psi) dz d\theta dx - \frac{1}{2} \\
& \times \int_{x_1}^{x_2} \int_0^{2\pi} \int_{-\frac{h}{2}-h_s}^{-\frac{h}{2}} \rho_p (\ddot{u} \delta u + \ddot{v} \delta v + \ddot{w} \delta w) x \sin(\psi) dz d\theta dx - \frac{1}{2} \\
& \times \int_{x_1}^{x_2} \int_0^{2\pi} \int_{\frac{h}{2}}^{\frac{h}{2}+h_a} \rho_p (\ddot{u} \delta u + \ddot{v} \delta v + \ddot{w} \delta w) x \sin(\psi) dz d\theta dx
\end{aligned} \tag{A-21}$$

For simplifying the above equation, Eq. (A-22) is considered.

$$I_0 = \int_{-\frac{h}{2}}^{\frac{h}{2}} \rho_m dz \tag{A-22.a}$$

$$I_0^s = \int_{\frac{h}{2}-h_s}^{-\frac{h}{2}} \rho_p dz \tag{A-22.b}$$

$$I_0^a = \int_{\frac{h}{2}}^{\frac{h}{2}+h_a} \rho_p dz \tag{A-22.c}$$

Therefore, Eq. (A-21) is simplified as:

$$\begin{aligned}
\delta T = & -\frac{1}{2} \int_{x_1}^{x_2} \int_0^{2\pi} (I_o + I_0^s \\
& + I_0^a) (\ddot{u} \delta u + \ddot{v} \delta v + \ddot{w} \delta w) x \sin(\psi) dz d\theta dx
\end{aligned} \tag{A-23}$$

As it is obvious, all of the above equation terms are arranged with the variation of displacement in three directions (δu , δv , δw) and these inertial terms will be presented in the final electromechanical equations of the conical shell.

In the next step work done by the external mechanical force is derived. For this purpose, distributed force in the longitudinal direction (q_x), circumferential direction (q_θ) and transverse direction (q_z) is considered. The work done by these distributed forces is calculated by:

$$W = \int_{x_1}^{x_2} \int_0^{2\pi} (q_x u + q_\theta v + q_z w) x \sin(\psi) dz d\theta dx \tag{A-24}$$

Considering this, the variation of external force work is extracted and presented in Eq. (A-25).

$$\delta W = - \int_{x_1}^{x_2} \int_0^{2\pi} (q_x \delta u + q_\theta \delta v + q_z \delta w) x \sin(\psi) dz d\theta dx \quad (\text{A-25})$$

Considering Eqs. (A-20), (A-23) and (A-25), all of the variation terms can be summed based on the Hamilton principle ($\delta T - \delta H = \delta w$). By this method, electromechanical equations of motion conical shells with sensor and actuator layer are extracted.

$$\begin{aligned} \delta u : & \frac{\partial}{\partial x} (N_{xx}^m + N_{xx}^{ms} + N_{xx}^{ma} - N_{xx}^e) \\ & + \frac{(N_{xx}^m + N_{xx}^{ms} + N_{xx}^{ma} - N_{xx}^e) - (N_{\theta\theta}^m + N_{\theta\theta}^{ms} + N_{\theta\theta}^{ma} - N_{\theta\theta}^e)}{x} \\ & + \frac{1}{x \sin(\psi)} \frac{\partial}{\partial \theta} (N_{x\theta}^m + N_{x\theta}^{ms} + N_{x\theta}^{ma}) + q_x \\ & = (I_o + I_o^s + I_o^a) \ddot{u} \end{aligned} \quad (\text{A-26.a})$$

$$\begin{aligned} \delta v : & \frac{\partial}{\partial x} (N_{x\theta}^m + N_{x\theta}^{ms} + N_{x\theta}^{ma}) + \frac{2}{x} (N_{x\theta}^m + N_{x\theta}^{ms} + N_{x\theta}^{ma}) + \frac{1}{x \sin(\psi)} \\ & \times \frac{\partial}{\partial \theta} (N_{\theta\theta}^m + N_{\theta\theta}^{ms} + N_{\theta\theta}^{ma} - N_{\theta\theta}^e) + \frac{\cos(\psi)}{x \sin(\psi)} \\ & \times \frac{\partial}{\partial x} (M_{x\theta}^m + M_{x\theta}^{ms} + M_{x\theta}^{ma}) + \frac{2 \cos(\psi)}{x^2 \sin(\psi)} (M_{x\theta}^m + M_{x\theta}^{ms} + M_{x\theta}^{ma}) \\ & + \frac{\cos(\psi)}{(x \sin(\psi))^2} \frac{\partial}{\partial \theta} (M_{\theta\theta}^m + M_{\theta\theta}^{ms} + M_{\theta\theta}^{ma} - M_{\theta\theta}^e) + q_\theta \\ & = (I_o + I_o^s + I_o^a) \ddot{v} \end{aligned} \quad (\text{A-26.b})$$

$$\begin{aligned} \delta w : & \frac{\partial^2}{\partial x^2} (M_{xx}^m + M_{xx}^{ms} + M_{xx}^{ma} - M_{xx}^e) + \frac{2}{x} \\ & \times \frac{\partial}{\partial x} (M_{xx}^m + M_{xx}^{ms} + M_{xx}^{ma} - M_{xx}^e) \\ & - \frac{\cos(\psi)}{x \sin(\psi)} (N_{\theta\theta}^m + N_{\theta\theta}^{ms} + N_{\theta\theta}^{ma} - N_{\theta\theta}^e) + \frac{1}{(x \sin(\psi))^2} \\ & \times \frac{\partial^2}{\partial \theta^2} (M_{\theta\theta}^m + M_{\theta\theta}^{ms} + M_{\theta\theta}^{ma} - M_{\theta\theta}^e) - \frac{1}{x} \\ & \times \frac{\partial}{\partial x} (M_{\theta\theta}^m + M_{\theta\theta}^{ms} + M_{\theta\theta}^{ma} - M_{\theta\theta}^e) + \frac{2}{x \sin(\psi)} \\ & \times \frac{\partial^2}{\partial x \partial \theta} (M_{x\theta}^m + M_{x\theta}^{ms} + M_{x\theta}^{ma}) + \frac{2}{x^2 \sin(\psi)} \\ & \times \frac{\partial}{\partial \theta} (M_{x\theta}^m + M_{x\theta}^{ms} + M_{x\theta}^{ma}) + q_z \\ & = (I_o + I_o^s + I_o^a) \ddot{w} \end{aligned} \quad (\text{A-26.c})$$

$$\delta \varphi : \frac{\partial}{\partial z} ((e_{31} \varepsilon_{xx} + e_{32} \varepsilon_{\theta\theta} + e_{33} E_z) x \sin(\psi)) = 0 \quad (\text{A-26.d})$$

If the actuator and sensor layer thickness is neglectable in comparison with conical shell thickness, then the electromechanical equations of motion will be simplified. In this case piezoelectric layer mechanical and inertial terms can be neglected and the electromechanical equations of motion can be written as:

$$\begin{aligned} \delta u : & \frac{\partial N_{xx}^m}{\partial x} + \frac{N_{xx}^m - N_{\theta\theta}^m}{x} + \frac{1}{x \sin(\psi)} \frac{\partial N_{x\theta}^m}{\partial \theta} + q_x \\ & = I_o \ddot{u} + \frac{\partial N_{xx}^e}{\partial x} + \frac{N_{xx}^e - N_{\theta\theta}^e}{x} \end{aligned} \quad (\text{A-27.a})$$

$$\begin{aligned} \delta w : & \frac{\partial N_{x\theta}^m}{\partial x} + \frac{2}{x} N_{x\theta}^m + \frac{1}{x \sin(\psi)} \frac{\partial N_{\theta\theta}^m}{\partial \theta} + \frac{1}{x \tan(\psi)} \frac{\partial M_{x\theta}^m}{\partial x} \\ & + \frac{2}{x^2 \tan(\psi)} M_{x\theta}^m + \frac{\cos(\psi)}{(x \sin(\psi))^2} \frac{\partial M_{\theta\theta}^m}{\partial \theta} + q_\theta \\ & = I_o \ddot{v} + \frac{1}{x \sin(\psi)} \frac{\partial N_{\theta\theta}^e}{\partial \theta} + \frac{\cos(\psi)}{(x \sin(\psi))^2} \frac{\partial M_{\theta\theta}^e}{\partial \theta} \end{aligned} \quad (\text{A-27.b})$$

$$\begin{aligned} \delta w : & \frac{\partial^2 M_{xx}^m}{\partial x^2} + \frac{2}{x} \frac{\partial M_{xx}^m}{\partial x} - \frac{N_{\theta\theta}^m}{x \tan(\psi)} + \frac{1}{(x \sin(\psi))^2} \frac{\partial^2 M_{\theta\theta}^m}{\partial \theta^2} - \frac{1}{x} \frac{\partial M_{\theta\theta}^m}{\partial x} \\ & + \frac{2}{x \sin(\psi)} \frac{\partial^2 M_{x\theta}^m}{\partial x \partial \theta} + \frac{2}{x^2 \sin(\psi)} \frac{\partial M_{x\theta}^m}{\partial \theta} + q_z \\ & = I_o \ddot{w} + \frac{\partial^2 M_{xx}^e}{\partial x^2} + \frac{2}{x} \frac{\partial M_{xx}^e}{\partial x} - \frac{N_{\theta\theta}^e}{x \tan(\psi)} + \frac{1}{(x \sin(\psi))^2} \frac{\partial^2 M_{\theta\theta}^e}{\partial \theta^2} \\ & - \frac{1}{x} \frac{\partial M_{\theta\theta}^e}{\partial x} \end{aligned} \quad (\text{A-27.c})$$

$$\delta \varphi : \frac{\partial}{\partial z} (e_{31} \varepsilon_{xx} + e_{32} \varepsilon_{\theta\theta} + e_{33} E_z) = 0 \quad (\text{A-27.d})$$

References

- [1] Li SDHH, Tzou HS, Chen ZB. Optimal vibration of conical shells with collocated helical sensor/actuator pairs. *J Theor Appl Mech* 2012.
- [2] Li F-M, Song Z-G, Chen Z-B. Active vibration control of conical shells using piezoelectric materials. *J Vib Control* 2012;18(14):2234–56.
- [3] Tzou HS, Chai WK, Wang DW. Modal voltages and micro-signal analysis of conical shells of revolution. *J Sound Vib* 2003;260(4):589–609.
- [4] Chai WK, Dehaven JG, Tzou HS. Spatial Microscopic Actuations of Shallow Conical Shell Sections. *J Vib Control* 2005;11(11):1397–411.
- [5] Chai WK, Han Y, Higuchi K, Tzou HS. Micro-actuation characteristics of rocket conical shell sections. *J Sound Vib* 2006;293(1-2):286–98.
- [6] Li H, Chen ZB, Tzou HS. Distributed actuation characteristics of clamped-free conical shells using diagonal piezoelectric actuators. *Smart Mater Struct* 2010;19(11):115015. <https://doi.org/10.1088/0964-1726/19/11/115015>.
- [7] Jamshidi R, Jafari AA. Evaluating actuator distributions in simply supported truncated thin conical shell with embedded piezoelectric layers. *J Intell Mater Syst Struct* 2018;29(12):2641–59.
- [8] Li H, Chen ZB, Tzou HS. Torsion and transverse sensing of conical shells. *Mech Syst Sig Process* 2010;24(7):2235–49.
- [9] Chai WK, Smithmaitre P, Tzou HS. Neural potentials and micro-signals of non-linear deep and shallow conical shells. *Mech Syst Sig Process* 2004;18(4):959–75.
- [10] Jamshidi R, Jafari A. Evaluating sensor distribution in simply supported truncated conical shells with piezoelectric layers. *Mech Adv Mater Struct* 2019;26(14):1179–94.
- [11] Jamshidi R, Jafari A. Transverse sensing of simply supported truncated conical shells. *J Comput Appl Mech* 2018;49(2):212–30.
- [12] Ghasemi FA, Ansari R, Paskiaby RB. Free vibration analysis of truncated conical composite shells using the Galerkin method. *J Appl Sci* 2012;12(7):698–701.
- [13] Li F-M, Kishimoto K, Huang W-H. The calculations of natural frequencies and forced vibration responses of conical shell using the Rayleigh–Ritz method. *Mech Res Commun* 2009;36(5):595–602.
- [14] Lam KY, Hua L. On free vibration of a rotating truncated circular orthotropic conical shell. *Compos B Eng* 1999;30:135–44.
- [15] Doghri I, Tiné L. Micromechanical modeling and computation of elasto-plastic materials reinforced with distributed-orientation fibers. *Int J Plast* 2005;21(10):1919–40.